Molecular and Cellular Mechanisms of Increased Angiogenesis in Multiple Myeloma: A Role for CXCL12

Sally K. Martin

Myeloma Research Group
Bone and Cancer Research Laboratory,
Division of Haematology,
Hanson Institute
Institute of Medical and Veterinary Science

&

Department of Medicine,
Faculty of Health Sciences
University of Adelaide

A thesis submitted to the University of Adelaide
for the degree of Doctor of Philosophy
December 2008

Chapter 1:

INTRODUCTION

1.1 An Overview

Multiple myeloma (MM) is an incurable haematological malignancy of unknown aetiology which affects plasma cells (PCs) of the bone marrow (BM) [1]. Depending on the stage at which MM is diagnosed and its response to treatment, patients have a median survival of approximately five years with current conventional therapy [2,3].

Among the clinical features of this disease is an increase in BM angiogenesis proximal to areas of PC infiltrate, which is a prognostic indicator of a poor prognosis [4-8]. The molecular mechanisms underlying the increased BM angiogenesis in MM are complex and have yet to be fully elucidated, however it is believed to be the product of numerous autocrine and paracrine interactions between MM PCs and neighbouring BM microenvironmental cells such as endothelial cells (ECs), BM stromal cells (BMSCs) and osteoclasts (OCs).

Previous findings from our laboratory have shown that the CXCL12 chemokine is aberrantly expressed by MM PCs [9]. Recent studies have also demonstrated that CXCL12 is a potent angiogenic factor [10-12] and is associated with angiogenesis in several biological systems [13,14]. The studies presented in this thesis were directed towards examining whether MM-derived CXCL12 is involved in angiogenesis in MM. Furthermore, as this study progressed, pioneering work was published by Ceradini *et al*, which demonstrated that CXCL12 expression is up-regulated by hypoxia [15]. Hypoxia, which is a state of decreased cellular oxygen availability, is a physiological feature of the BM microenvironment and importantly, is a known stimulus for tumour angiogenesis. With this knowledge, the focus of this project evolved to encompass a detailed examination of hypoxia as a potential mediator of aberrant CXCL12 expression in MM PCs. Altogether, this research was conducted with the intention of adding to our current understanding of the underlying mechanisms of increased angiogenesis in MM, and to identify putative therapeutic targets.

The introduction section which follows represents a brief overview of the literature regarding (i) the biology of MM, (ii) the process of angiogenesis and its role in tumour pathogenesis, (iii) the role of CXCL12 in normal and tumour biology, and (iv) hypoxia and its role in tumorigenesis.

1.2 Multiple Myeloma

1.2.1 General Description

MM is characterised by the "homing" of a clonal population of neoplastic PCs from secondary lymphoid organs to congenial sites within the BM microenvironment [1] (Figure 1.1). The main clinical manifestations of MM are the development of devastating osteolytic bone lesions at multiple sites throughout the skeleton, bone pain, hypercalcemia, increased plasma volume, renal insufficiency, suppressed immunoglobulin production and increased BM angiogenesis [16]. MM encompasses a spectrum of clinical variants ranging from smouldering or indolent myeloma to more aggressive, disseminated forms of MM and PC leukaemia.

The MM PC is characterised by marked heterogeneity in morphology, immunophenotype and genetic abnormality [17-20]. As a result, a detailed assessment of the pathological, radiological and clinical features of the disease is required to diagnose and assess the stage and activity of MM in individual patients. The prognosis, clinical course and response to therapeutic intervention varies greatly between MM patients, as highlighted by the fact that although the median overall survival of MM patients is five years with current conventional therapy [3], it ranges from less than six months to greater than ten years [2,21].

Studies to date have been unable to identify any causative factors for the development of MM, and it appears likely that several environmental and predisposing genetic factors are involved. MM is characterised by extensive genetic disorder [22,23], and the accumulation of numerous chromosomal mutations are believed to contribute to the development of the disease [24]. While factors such as exposure to radiation and certain chemicals have also been implicated, the diversity of these exposures has made a definitive assessment impossible.

1.2.2 Epidemiology

MM accounts for approximately 1% of all cancers and 15% of haematological cancers, and is the second most common haematological malignancy after non-Hodgkin's lymphoma (NHL) [16,25]. MM predominantly affects the middle-aged or elderly, as reflected by a median age at diagnosis of 69 years in men and 71 years in women [26]. Furthermore, almost 80% of all new cases in Australia are diagnosed in persons over the age of 60 [25] and in a large epidemiological study of MM patients diagnosed at the Mayo Clinic in America

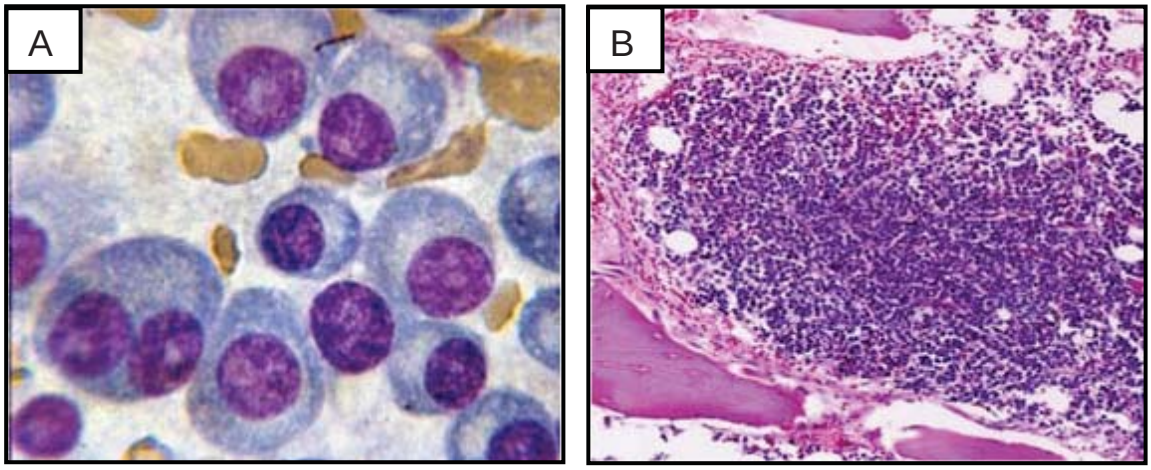

Figure 1.1. Myeloma Plasma Cells. (**A**) A bone marrow smear taken from a MM patient which shows the presence of abnormal plasma cells. (**B**) A trephine biopsy derived from the iliac crest of a patient with advanced MM, in which the uncontrolled proliferation of MM plasma cells has almost completely replaced the normal haemopoietic bone marrow tissue.

(Rochester, Minnesota) between 1956-1995, 12% of the 4081 MM patients were younger than 50 years and only 2% were aged less than 40 years [27].

The incidence of MM varies by race and geographic location, ranging from one patient per hundred thousand in China to six patients per hundred thousand in Western industrialised countries each year [16]. Each year in Australia, approximately 1,100 people are diagnosed with MM at an incidence of 5.8 patients per hundred thousand [25]. While the incidence in African Americans is more than twice that of Caucasians, and slightly more men than women are afflicted [16,25], to date, epidemiological studies have been unable to account for these apparent racial and gender differences. The incidence of MM has steadily increased over time due to better diagnostic techniques, increasing survival times in response to improved therapeutic options, and the rising average age of the general population. Alarmingly, the latest epidemiological survey released by the Australian Institute of Health and Welfare reported a 44% increase in the number of Australians diagnosed with MM in 2003 compared to 1993 [25].

1.2.3 Clinical Variants of Multiple Myeloma

Plasma cell dyscrasias encompass a spectrum of pre-malignant and malignant conditions (Table 1.1). A relatively common benign PC tumour called monoclonal gammopathy of undetermined significance (MGUS) often precedes the onset of MM. MGUS is a B-cell disorder which affects approximately 3% of the normal population aged over 50 years and 5% of people aged over 70 years [28]. Every year, approximately 1% of MGUS patients will progress to MM or another related haematological disorder [29], however 75% of MGUS patients will remain without progression for over 20 years [30]. Like MM, MGUS involves the clonal proliferation of B-cells which produce a homogeneous monoclonal protein (M-protein, or paraprotein). However, unlike MM, MGUS is not associated with any local or systemic disorder and patients do not exhibit any of the debilitating symptoms associated with MM. Consequently, MGUS can remain undiagnosed for many years. Studies suggest that approximately 20-25% of MGUS patients will eventually progress to MM, amyloidosis or NHL [31]. The precise events that lead to the development of MGUS and its transformation into secondary conditions are yet to be determined.

Non-secretory MM accounts for approximately 1% of all cases and is characterised by the presence of malignant PCs that do not produce any M-protein [1]. Smouldering or indolent

Table 1.1. The Spectrum of Plasma Cell Dyscrasias

Clinical Variant	Definition
MGUS (monoclonal gammopathy of undetermined significance)	Monoclonal protein present with marrow plasmacytosis < 10% but not associated with underlying disease. No myeloma-related symptoms.
Smouldering or Indolent Myeloma	As per MGUS but with evidence of increasing M-protein levels and marrow plasmacytosis 10-30%. Still no myeloma-related symptoms.
Active Myeloma	Monoclonal protein present with marrow plasmacytosis > 30% and the presence of lytic bone lesions.
Plasma Cell Leukaemia	As per active myeloma but plasma cells have entered the peripheral blood at concentrations of $>2x10^9$/litre or >20% of the differential white blood cell count.

myeloma is a variant in which the diagnostic criteria for MM are met, but the patient is asymptomatic and therefore does not require treatment. The progression of smouldering or indolent MM to active MM is associated with increasingly severe secondary features such as osteolytic bone lesions, anaemia, immunodeficiency and renal impairment. In a small number of patients, MM can progress to an extramedullary state in which malignant MM PCs develop into tumours outside of the bone, commonly in areas such as the blood, skin and pleural fluid [22]. Extramedullary MM is the most aggressive PC dyscrasia, and when it involves the blood, is often called PC leukaemia.

Historically, the diagnosis of active MM was dependent upon the presence of increased numbers of BM PCs (>10%), M-protein (>3g/dL) in the blood or urine, and osteolytic bone lesions at one or more sites throughout the skeleton [32]. The staging of MM generally required consideration of both the number and specific properties of MM PCs in a given patient and until recently, this was performed with reference to the international Durie and Salmon staging system (Table 1.2). Developed in 1975, the Durie and Salmon staging system divided MM into three stages based on clinical parameters such as the total number of MM PCs in the body, serum calcium levels, the number of osteolytic bone lesions, and M-protein value [32].

In an effort to devise a simpler, more objective diagnostic classification system for MM patients, clinicians from around the world recently pooled data from 10,750 newly-diagnosed MM patients and evaluated numerous potential prognostic factors to devise a new staging system [2]. The results of this study culminated in the development of the International Staging System (ISS) for MM, developed in 2005 (Table 1.3). The ISS classifies patients on the basis of the results from two simple blood tests, beta-2-microglobulin (β2M) and serum albumin, which together were found to have the greatest prognostic power in MM patients [2].

Beyond the Durie and Salmon and ISS, researchers are attempting to move towards molecular fingerprinting as a basis for classifying MM patients. Conventional cytogenetic karyotyping is emerging as a relevant prognostic tool and studies to date have found that, of the many chromosomal gains and losses associated with the development of MM, deletion of chromosome 13 is the most common and is a strong prognostic indicator of clinical outcome [33,34]. Similarly, microarray analysis of global gene expression patterns is a

Table 1.2. The Durie and Salmon Staging System for Multiple Myeloma [32]

Stage I (low cell mass)
All of the following:

- Haemoglobin value > 10 GM/DL
- Serum calcium value normal or < 10.5 mg/DL
- Bone X-ray, normal bone structure (scale 0) or solitary bone plasmacytoma only
- Low M-component production rates
  IgG value < 5.0 GM/DL
  IgA value < 3.0 GM/DL
  Urine light chain M-component on electrophoresis < 4 GM/24h
- Measured myeloma cell mass (billions/m2) - 600 billion*

Stage II (intermediate cell mass)
Fitting neither stage I nor stage III.

- Measured myeloma cell mass (billions/m2) - 600 to 1,200 billion*

Stage III (high cell mass)
One or more of the following:

- Haemoglobin value < 8.5 GM/DL
- Serum calcium value > 12 mg/DL
- Advanced lytic bone lesions (scale 3)
- High M-component production rates
  IgG value > 7.0 GM/DL
  IgA value > 5.0 GM/DL
  Urine light chain M-component on electrophoresis >12 GM/24h
- Measured myeloma cell mass (billions/m2) > 1,200 billion*

Subclassification (either A or B)

- **A**: relatively normal renal function
  (serum creatinine value) < 2.0 mg/DL
- **B**: abnormal renal function
  (serum creatinine value) > 2.0 mg/DL

Examples: Stage IA (low cell mass with normal renal function)
Stage IIIB (high cell mass with abnormal renal function)

* myeloma cells in the whole body

Table 1.3. The International Staging System (ISS) for Multiple Myeloma [2]

NOTE:
This table is included in the print copy of the thesis held in the University of Adelaide Library.

powerful means of identifying clinical subgroups of haemopoietic malignancies [18,35]. In MM, microarray technology has been used to classify patients into subgroups according to their genetic profile and correlations between specific profiles and clinical characteristics examined. These studies represent the framework for extending current classification systems for MM patients and provide the foundation for using genetic profiling to determine the optimal treatment regimes for individuals with MM.

1.2.4 Clinical Features of Multiple Myeloma

The uncontrolled expansion of the MM PC clone in the BM leads to the gradual displacement of normal haemopoietic function, which has severe consequences for MM patients. In addition, MM PC accumulation in the BM microenvironment results in the secretion of a homogeneous M-protein which causes the suppression of normal immunoglobulin production, amyloidosis, renal insufficiency, increased plasma volume, and anaemia. These occurrences lead to a significantly reduced quality of life and inevitably death. A free light chain immunoglobulin, known as Bence-Jones protein, is present in the urine of approximately 75% of patients and renal tubular re-absorption of this protein is largely responsible for the kidney damage that occurs in MM [1].

The prominent clinical feature of MM is the occurrence of destructive skeletal events: lytic bone lesions, pathological fractures, and nerve compression syndromes [1,36,37] (Figure 1.2). Many patients present with bone pain as their predominant symptom [36], and approximately 50% of patients exhibit vertebral fractures at diagnosis [38]. In most patients, multiple lytic lesions and pathological fractures develop throughout the skeleton, commonly in the pelvis, spine, ribs, shoulders and skull. These events are caused by the aberrant activity of bone-resorbing osteoclasts (OCs) at sites of MM PC infiltration. Intriguingly, the destructive bone resorption that occurs in MM is seemingly irreversible, with studies demonstrating that lytic bone lesions rarely heal, even when patients are in complete remission [39]. Osteolysis in MM patients causes a continual loss of calcium from the skeleton leading to hypercalcemia, or elevated serum calcium levels, which causes further clinical complications such as dehydration and renal insufficiency.

As discussed in detail in Section 1.3.5, another clinical feature associated with active MM is excessive BM angiogenesis [4-8], a feature common to numerous haematological malignancies and solid tumours [40,41] (Figure 1.3). Angiogenesis contributes to the

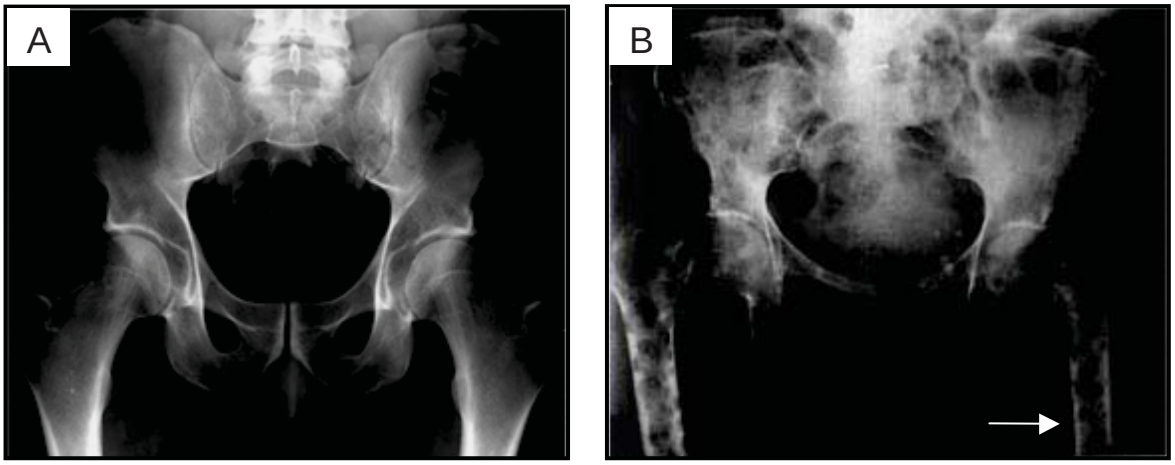

Figure 1.2. Osteolytic Bone Disease in Multiple Myeloma Patients. A radiograph of the pelvic girdle and femora of (**A**) an age-matched healthy individual and (**B**) a patient with MM. Note the typical "punched out" osteolytic bone lesions in the myeloma skeleton (arrow).

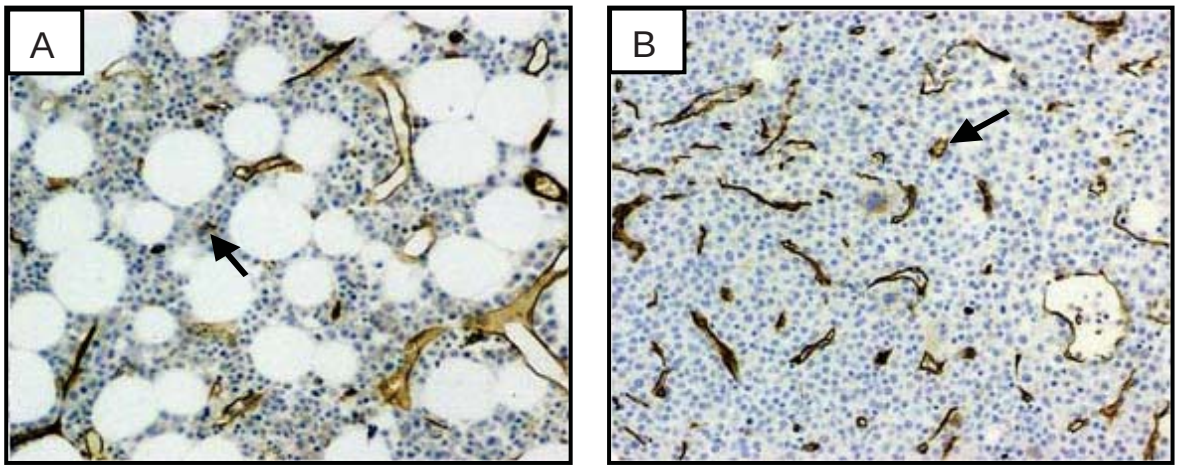

Figure 1.3. Immunohistochemical Microvessel Staining of Patient Bone Marrow Trephines. Anti-CD34 endothelial staining of blood vessels (arrows) in paraffin-embedded trephine sections derived from the iliac crest of (**A**) an age-matched healthy individual and (**B**) a MM patient (original x200 magnification). Sections were counterstained with haematoxylin. Note the increased microvessel density in the myeloma patient section, stained red by CD34 endothelial staining

pathogenesis of MM by providing an abundant oxygen and nutrient supply to facilitate tumour growth. In addition, angiogenesis enables paracrine stimulation of tumour cell migration and proliferation and provides passage for bone-resorbing OCs to move throughout the skeleton [42].

1.2.5 Treatment

Due to the highly variable nature of the disease, there is no single 'standard therapy' for patients with MM. Instead, individual treatment plans are prepared with reference to the patient's age, general health, symptoms, and disease status. Treatment strategies for MM can be divided into two categories: definitive or supportive. Definitive therapies target the underlying disease with the intention of bringing about a full or partial remission and extending the patient's survival time. Definitive treatment measures include alkylating chemotherapeutic agents such as cyclophosphamide, vincristine, doxorubicin and melphalan, and transplant-based therapies such as autologous or allogeneic BM and stem cell transplants. Supportive or palliative treatments are directed towards controlling the effects of the disease on other tissues and organs, with the intention of improving the patient's quality of life. Supportive treatment measures include blood and platelet transfusions to replenish depleted haemopoietic cells, bisphosphonates to treat hypercalcemia and prevent MM bone disease [43], vertebroplasty and kyphoplasty to treat vertebral fractures, and prophylactic antibiotics to prevent infection in immunosuppressed patients.

From the 1960's until very recently, conventional therapy for MM patients consisted of alkylating agents in combination with glucocorticoids, with melphalan plus prednisone considered the gold standard treatment [44]. However, due to recent significant advances in our understanding of MM biology, a number of exciting new drugs have emerged and have shifted old treatment paradigms. Over the last ten years, immunomodulatory drugs such as thalidomide [45] and lenalidomide [46,47] and the proteasome inhibitor, bortezomib [48,49] have emerged as highly active agents in the treatment of MM and have revolutionised MM therapy. Ongoing studies are currently examining various combinations of these new drugs with conventional chemotherapeutics in newly-diagnosed, relapsed or refractory MM patient groups. Preliminary results are showing promising improvements in complete response rates and it is anticipated that these drugs will dramatically improve patient survival times [49-53]. Already, the latest statistics indicate that the 5-year survival rate for a

newly-diagnosed patient in Australia is 34% [54], up from 26% 30 years ago [54]. In addition, a number of other novel therapeutic agents which target MM PCs and their interactions with the BM microenvironment are currently undergoing clinical trials and are likely to further improve patient outcomes [55].

1.3 Molecular Mechanisms of Physiological Angiogenesis

1.3.1 The Physiology of a Healthy Vascular System

The cardiovascular system carries oxygenated blood from the heart to every tissue and cell of the body via a complex organisation of blood vessels composed of large arteries, which feed into smaller arterioles and subsequently into capillary beds [56]. Capillary beds are extensive mesh-like networks which ultimately deliver the blood to the most distant cells of the body and facilitate the exchange of gases and metabolic products between the blood, cells and tissues. De-oxygenated blood from these tissues and cells is then returned to the heart via venules and veins, sent to the lungs for re-oxygenation and returned to the heart to begin the cycle again [56]. To adapt to changing metabolic circumstances, arteries and veins generally expand via circumferential growth and remodelling, whereas capillaries undergo sprouting and branching into more complex networks [57].

The most fundamental component of the vascular system is the endothelial cell (EC). Every blood vessel in the human body, from the major aorta through to the smallest capillary, consists of an EC monolayer which encases a central lumen through which the blood flows. The EC monolayer, or vascular endothelium, is a dynamic organ which has vital secretory and metabolic functions and controls the trafficking of cells and molecules between all bodily tissues, the circulatory system and the BM [58]. Structurally, the endothelium is supported by a basement membrane scaffold consisting of laminin and collagen protein fibres and, in larger vessels, peri-vascular support cells such as pericytes and smooth muscle cells. Separating large blood vessels from surrounding tissues is a layer of connective tissue called the stroma, which is principally composed of extracellular matrix (ECM)-secreting fibroblasts.

Due to the absolute necessity for oxygen, all mammalian cells must be located within 100 - 200μm of the blood vessel network, a distance which corresponds to the diffusion limit for oxygen [59]. The formation and remodelling of the vascular system can be divided into two separate processes: vasculogenesis and angiogenesis. Vasculogenesis denotes the

de novo formation of the primitive vascular system through the differentiation of mesodermal angioblasts [60], whereas angiogenesis denotes the formation of new blood vessels from pre-existing vasculature through the sprouting or invagination of existing vessels [61]. Until recently, vasculogenesis was believed to be restricted to early embryonic development, however recent studies have demonstrated that circulating endothelial progenitor cells are present in the peripheral blood circulation and contribute to physiological and pathological vasculogenesis in adulthood [62].

1.3.2 Angiogenesis

Angiogenesis is an essential part of both embryonic development and maintenance processes such as wound healing, inflammation and female reproductive function throughout adult life [14,61,63]. Angiogenesis occurs via two distinct mechanisms: sprouting and intussusception. Each mechanism is markedly different from the other: sprouting angiogenesis is the formation of entirely new vessels from pre-existing vasculature [64], whereas intussusceptive angiogenesis is the splitting of a larger "mother" vessel into smaller "daughter" vessels through the insertion of tissue pillars [65-67]. Both mechanisms of angiogenesis have been reported to occur under normal and pathological conditions [68,69].

To date, the most defined mechanism of angiogenesis is sprouting angiogenesis. First described by Ausprunk and Folkman in the 1970's [64], sprouting angiogenesis is a tightly coordinated, multi-step process encompassing phases of EC proliferation, differentiation, migration and matrix adhesion. Under normal conditions, sprouting angiogenesis is a self-limited process which can take days (eg. ovulation), weeks (eg. wound healing) or months (eg. placentation) to complete, depending on the circumstance [70]. As depicted in Figure 1.4, sprouting angiogenesis follows an orderly series of events, and begins with the production and secretion of angiogenic growth factors by diseased or injured tissues, which diffuse outwards through adjacent tissues. These growth factors bind to EC receptors within nearby blood vessels, initiating internal signal transduction cascades which result in the flipping of cellular polarity, the induction of motile and invasive activity and the production of matrix-degrading enzymes. These enzymes focally degrade the basement membrane of the blood vessel, facilitating the migration of proliferating ECs out into the surrounding tissue, following a gradient of pro-angiogenic cytokines and growth factors. Specialised adhesion molecules at the EC-ECM interface, such as integrins $\alpha_v\beta_3$, $\alpha_v\beta_5$ and $\alpha_5\beta_1$, also guide the newly sprouting vessel forward. As the sprouting vessel extends, the

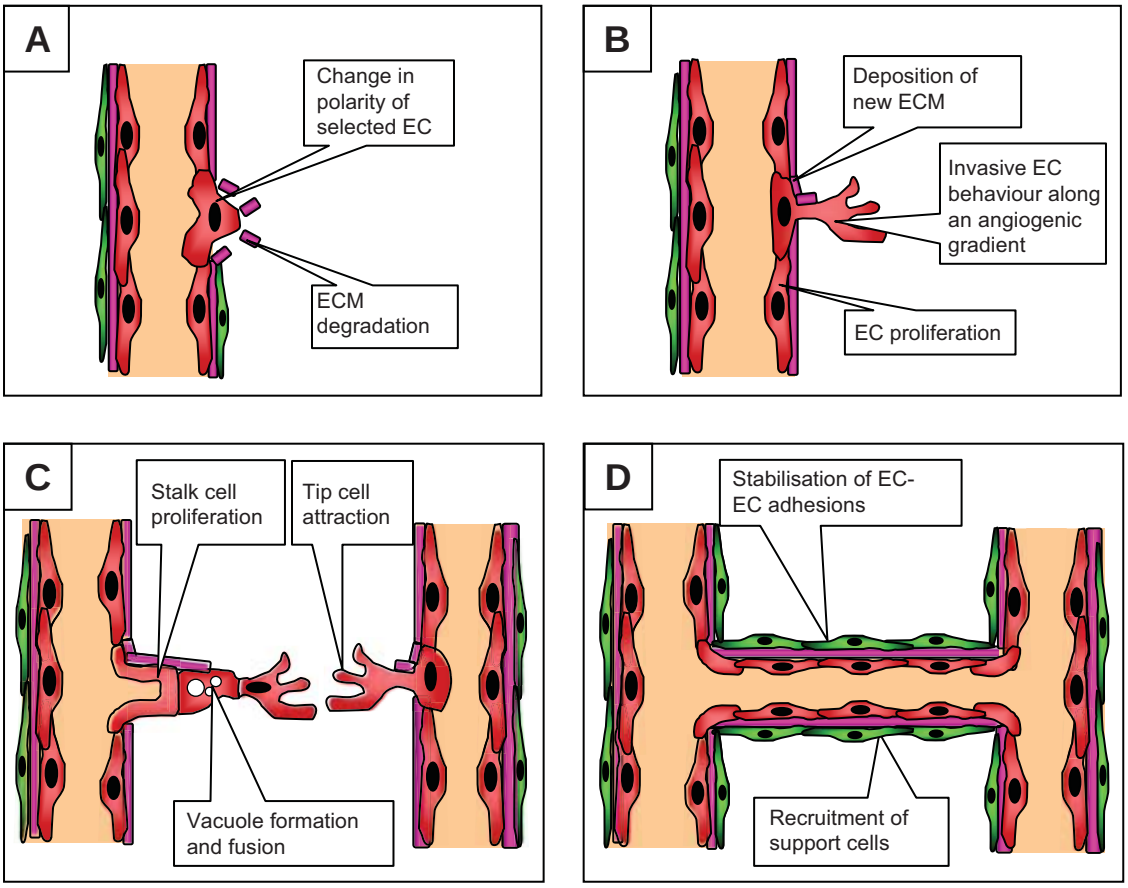

Figure 1.4. The Process of Sprouting Angiogenesis. (**A**) Under favourable pro-angiogenic conditions, ECs within pre-existing vessels are activated and selected for angiogenic sprouting. In these activated ECs, the apical-basal cell polarity is reversed and matrix-degrading enzymes are produced. These enzymes focally degrade the basement membrane of the blood vessel, facilitating the migration of proliferating ECs out into the surrounding tissue. (**B**) The proliferating sprout is guided along a gradient of pro-angiogenic cytokines, aided by specialised adhesion molecules such as integrins. As the sprouting vessel extends, new extracellular matrix is deposited around it. (**C**) Sprouting ECs are attracted to adjacent sprouts and connected by strong junctional contacts to form tubules. Lumen formation involves the fusion of internal vacuoles. (**D**) The establishment of a vascular lumen facilitates blood flow and stabilises the new vascular connections. The newly-formed blood vessel receives further re-inforcement with the recruitment of supportive cells such as pericytes and smooth muscle cells and extracellular matrix. Figure adapted with permission [57].

tissue is remodelled around it and sprouting ECs come together through strong EC-EC junctional contacts to form tubules. The establishment of a vascular lumen, via pinocytosis, facilitates blood flow and stabilises the new vascular connections. Finally, the newly-formed blood vessel is structurally stabilised by the recruitment of supportive cells such as pericytes and smooth muscle cells (SMCs) and the synthesis of ECM proteins such as fibronectin, laminin, and collagen Types I, III, V and VIII [71,72]. Sprouting angiogenesis is a relatively slow process, requiring more than 24 hours and at least three to five days before the newly formed vessel becomes properly perfused and integrated into the vascular network [64,73].

Compared to sprouting angiogenesis, little is known about the physiological role of intussusceptive angiogenesis [74]. Also known as "splitting" angiogenesis, intussusception occurs when the capillary wall extends into the lumen to split a single existing vessel into two. As depicted in Figure 1.5, the process begins when two opposing capillary walls establish an area of contact, causing a reorganisation of local intercellular EC junctions and the central perforation of vessel layers to facilitate the entry of growth factors and cells into the lumen. At this central area of contact, a transluminal pillar with an interstitial core is formed between the two new vessels, which is soon invaded by pericytes and myofibroblasts and rapidly enlarged through the deposition of collagen fibres. In the final phases, the pillar increases in size without any further change to the basic structure, which creates an internal division in the vessel and splits it into two [65,75]. Intussusceptive angiogenesis occurs much more rapidly than sprouting angiogenesis, requiring as little as two to five hours for complete transluminal pillar insertion [65,76]. Intussusceptive angiogenesis has been reported in a number of normal and malignant tissues, and facilitates a rapid increase in the complexity and density of a blood vessel network, independent of EC proliferation [68,77].

It is important to emphasise that vasculogenesis, sprouting angiogenesis and intussusceptive angiogenesis are not mutually exclusive mechanisms of blood vessel formation. Instead, it is thought that these processes are interlinked and act concurrently in both physiological and pathological situations.

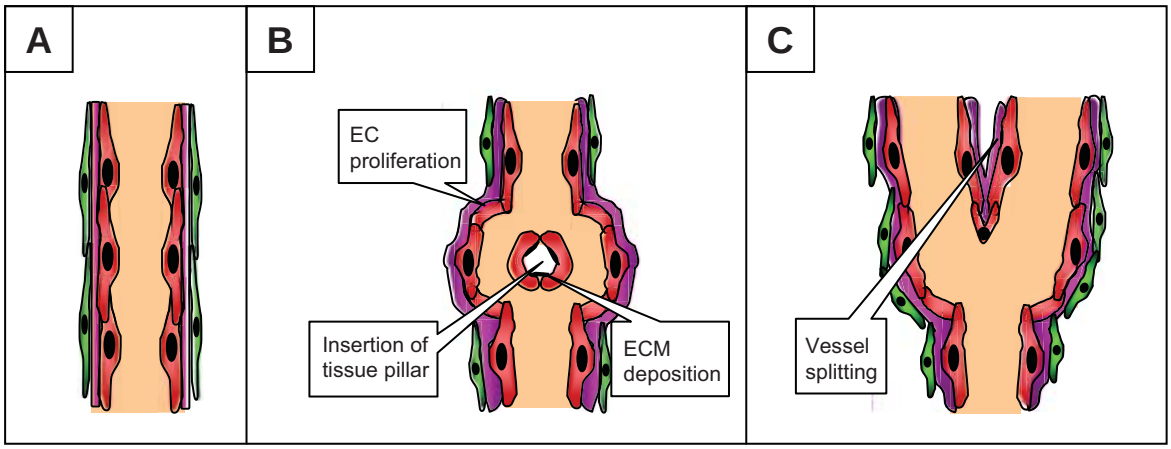

Figure 1.5. The Process of Intussusceptive Angiogenesis. (**A** and **B**) Upon initiation of intussusceptive angiogenesis, two opposing capillary walls establish an area of contact, causing a reorganisation of local intercellular EC junctions and the central perforation of vessel layers to facilitate the entry of growth factors and cells into the lumen. At this central area of contact, a transluminal pillar with an interstitial core is formed between the two new vessels, which is invaded by pericytes and myofibroblasts and rapidly enlarged through the deposition of collagen fibres. (**C**) The pillar then increases in size without any further change to the basic structure, leading to the creation of an internal division in the vessel thus splitting the vessel into two. Figure adapted with permission [57].

1.3.3 The Angiogenic Switch

ECs are one of the longest living cell types in the body outside of the central nervous system. They are genomically very stable and are largely quiescent throughout adulthood, with only 0.01% of ECs in a normal adult vessel undergoing cell division at any given time [78,79]. Even though most blood vessels remain quiescent throughout adulthood, ECs are able to divide rapidly in response to physiological stimuli, and these activating stimuli play a critical role in the initiation of pathological angiogenesis [80,81]. Important pro-angiogenic factors which mediate EC development, organisation and growth include vascular endothelial growth factor (VEGF), basic fibroblast growth factor (bFGF), platelet-derived growth factor (PDGF), granulocyte colony stimulating factor, interleukin-1 and -6 (IL-1 and IL-6), matrix metalloproteinases (MMPs), and angiopoietin (Ang)-1 [82,83]. VEGF and bFGF are essential for the initiation of vascular development, and in conjunction with Ang-1 and hepatocyte growth factor (HGF), are also involved with EC proliferation, survival and migration [84].

According to the widely accepted "angiogenic switch" model, the onset of angiogenesis is dependent on a local net imbalance between angiogenic (angiogenesis-promoting) and angiostatic (angiogenesis-inhibiting) stimuli [85]. The term 'angiogenic stimuli' encompasses growth factors (eg. VEGF), enzymes (eg. cathepsin K), trace elements (eg. copper), oncogenes (eg. c-myc, ras), cytokines (eg. interleukins), and cellular stresses (eg. low pH, hypoxia) [86]. A crucial difference between tumour-associated angiogenesis and physiological angiogenesis is that tumour angiogenesis does not result in the "switching off" of the angiogenic switch. Under normal conditions, the maturation of newly-formed vessels is met with the restoration of a net balance between angiogenic and angiostatic factors, and ECs return to a quiescent state [87]. During tumour angiogenesis, the net balance between angiogenic and angiostatic factors is never completely restored and thus the angiogenic switch remains "turned on". The prolonged and uncoordinated activation of tumour angiogenesis results in the formation of immature and unstable blood vessels which are irregular and leaky [88,89].

1.3.4 Angiogenesis in Cancer

Angiogenesis contributes to the development and progression of several pathological conditions, including cancer and autoimmune responses [69]. In 1945, Algire and Chalkley first observed that the growth of a solid tumour is closely associated with a vascular

network [90]. Since this initial observation, angiogenesis has been found to facilitate the development, progression and metastasis of solid tumours and is associated with a poor clinical outcome [91,92]. A solid tumour's requirement for nutrients and oxygen grows in proportion to its volume, but its ability to absorb these factors from the surrounding tissue is proportional to its surface area [93]. This, therefore, imposes a maximum size to which a solid tumour can grow before it experiences nutrient deficiency. It is generally accepted that the limited diffusion distances for oxygen and nutrients between cells restrict the size of solid tumours to 1-2mm in diameter [91]. To counteract this, tumour cells stimulate the growth of new blood vessels to enhance their blood supply and facilitate the transition from a growth-restricted state to an invasive phenotype. Tumour-induced angiogenesis provides an increased supply of oxygen, nutrients and pro-survival factors to facilitate the proliferation of the cancer cells, a system for the removal of waste products, and a vascular route for spread and expansion of metastases to secondary sites. Moreover, growth factors released from the endothelium itself stimulate tumour cell proliferation and migration.

Angiogenesis is associated with the progression of many solid tumours, including breast cancer [94-97], rectal carcinoma [98], prostate cancer [99], melanoma [100], and hepatocellular carcinoma [101-104]. Until recently, it was assumed that the importance of angiogenesis in solid tumours did not extend to haematological cancers. However, pioneering studies by Vacca *et al* [4] and others have demonstrated that angiogenesis is involved in the progression of several haematological malignancies, including MM [4,6-8], acute lymphoblastic leukaemia (ALL) [105-107], acute myeloid leukaemia (AML) [105,108,109], chronic myeloid leukaemia (CML) [105,110], chronic lymphoblastic leukaemia (CLL) [111], myelodysplastic syndrome (MDS) [112], and NHL [113,114].

1.3.5 Angiogenesis in Multiple Myeloma

In MM, the immunohistochemical assessment of BM microvessel density (MVD) in BM biopsy specimens provides a direct measure of the degree of angiogenesis. In 1994, Vacca *et al* demonstrated, for the first time, that the degree of BM angiogenesis is significantly greater in patients with active MM than in patients with MGUS and non-active MM [4]. These findings indicated that increased BM MVD is associated with a poor prognosis and clinical outcome, similar to tumour angiogenesis in solid cancers. Morphologically, the BM microvasculature in biopsies from active MM patients is tortuous and thin [4], mirroring the classical features of solid tumour angiogenesis [88,89]. Using larger

patient cohorts, subsequent studies have confirmed that an elevated BM MVD is associated with active MM [5-8]. Moreover, BM MVD has also been associated with other disease parameters such as BM PC infiltration (defined as the percentage of MM PCs in the BM) [115,116], PC labelling index [6], serum β2M levels [115,116] and overall survival [6-8]. A relationship between BM MVD and the presence of circulating PCs has also been demonstrated in MM patients [117].

The molecular mechanisms underlying the progressive increase in angiogenesis in MM are complex and have yet to be fully elucidated. However, it is clear that this process is governed by angiogenic factors produced both directly by MM PCs themselves and indirectly by BM microenvironmental cells such as BMSCs, OCs and ECs in response to the MM PCs [118,119]. MM PCs express numerous angiogenic factors, including VEGF [118,120,121], bFGF [122-125], HGF [126] and Ang-1 [84]. Soluble levels of VEGF, bFGF and HGF are elevated in the BM of patients with active MM compared to healthy individuals [125,127], however elevated levels of these angiogenic factors do not singularly correlate with disease severity and progression. This suggests that these angiogenic factors regulate angiogenesis collectively rather than singularly.

Using *in vitro* colony formation assays to assess the propensity of BM mononuclear cells to form endothelial colonies (CFU-En), studies have demonstrated that BM mononuclear cells from previously untreated MM patients form significantly greater numbers of CFU-En compared to normal and MGUS samples [128]. These data indicate that there is an increased angiogenic "potential" associated with MM, with a greater number of colony-forming EC progenitors present in the BM of patients with active MM compared healthy individuals and MGUS patients [128].

It is widely accepted that tumour endothelium is phenotypically and genotypically distinct from normal endothelium, particularly in terms of the expression of adhesion molecules, signalling receptors, proteases, and the structural proteins which comprise the basement membrane [129-132]. In line with this, ECs derived from the BM of MM patients (MM ECs) display important morphological, genetic and functional differences indicative of an angiogenic phenotype when compared to healthy, quiescent ECs [133]. These differences include: (i) elevated protein expression of the angiogenic receptors VEGFR2, Tie2 and bFGFR2; (ii) reduced protein expression of the angiogenesis inhibitor, thrombospondin;

(iii) increased β_3 integrin expression, which prevents EC apoptosis and facilitates EC adhesion to the matrix; (iv) increased *in vitro* proliferation, migration, capillarogenesis and *in vivo* angiogenesis in the chorioallantoic membrane (CAM) assay; and (v) increased gene expression of the angiogenic growth factors bFGF and VEGF [133].

In addition to the tumour endothelium, MM PCs themselves display a heightened angiogenic potential, as assessed in the chick embryo CAM assay using conditioned media (CM) from primary patient MM PCs [134]. In these studies, the PC CM of 20/26 (76%) active MM patient samples induced a profound angiogenic response, in contrast to only 4/20 (20%) of MGUS samples [134]. Furthermore, the PC CM from active MM patients was found to strongly induce *in vitro* EC proliferation and chemotaxis, and because similar numbers of PCs were assayed for each patient, these effects were attributed to the activity of the MM PCs rather than tumour burden [134].

1.4 The Chemokine System

Chemokines are small molecular weight (8-14 kDa) chemotactic proteins which signal through cell-surface G-protein coupled receptors. By definition, the predominant feature of these molecules is their ability to induce gradient-dependent chemotaxis, or directed cell migration. Chemokines play a key role in numerous biological processes including embryogenesis [135,136], haemopoiesis [137,138], leukocyte homeostasis [139], lymphoid organ development [140], cell trafficking [141-143], wound healing [144], inflammation [145,146], angiogenesis [147,148], HIV pathogenesis [149], Th1/Th2 polarisation [150] and tumour metastasis [151-153].

Structurally, chemokines are divided into four subfamilies based on the sequence motif around four conserved N-terminal cysteine residues - CXC, CC, C, or CX3C. Between the first two cysteine residues, the CC, CXC, and CX3C chemokines contain 0, 1, and 3 non-conserved amino acid residues respectively, whereas the C chemokines lack the first and third of the four conserved cysteine residues [154]. Chemokine receptors are named based on the chemokine class to which they bind, and a degree of redundancy exists within each subfamily, with many receptors binding to more than one ligand and many ligands able to bind to more than one receptor. However, this redundancy does not necessarily confer duplicity in function because ligands exhibit variable affinities for the

same receptor, and activate different signal transduction pathways and cellular responses [155].

To date, the human chemokine system consists of approximately 50 ligands and 18 receptors. In many cases, chemokines have been designated multiple names over the years. To simplify matters, Zlotnik *et al* devised a new nomenclature system for all chemokines (Table 1.4), in which the chemokine structural code (CXC, CC, CX3C or C) is followed by 'L' for ligands or 'R' for receptors and then a number [156].

Based on function and patterns of expression, chemokines can be broadly classed as either 'inflammatory' or 'homeostatic'. Inflammatory chemokines are inducible, mediate inflammatory and immune responses [157] and bind to multiple receptors. Conversely, homeostatic chemokines are constitutively expressed, mediate homeostatic processes of the haemopoietic and immune systems, and generally bind to a single receptor. However, it has become clear that several chemokines do not exclusively belong to either of these groups, but instead share characteristics of both. These chemokines are termed 'dual function' chemokines [158].

The majority of chemokines are produced and stored within the secretory apparatus of the synthesizing cell, ready for rapid release upon cell activation [159]. The exceptions to this are CXCL16 and CX3CL1, which are produced as membrane-bound proteins and act as cell adhesion molecules unless they are released from the cell surface by proteolytic enzymes [160,161]. These secreted chemokines are subsequently immobilised on the ECM or cell surface by glycosaminoglycans.

Binding of chemokines to their respective receptors initiates a multitude of intracellular signalling cascades, including protein kinase C, phospholipase C, phosphoinositide-3-kinase (PI3K) and various src family kinases [162]. These signalling cascades lead to the activation of Rac and Rho, whose reciprocal activation and inactivation at the leading and trailing edge of the cell mediates its directional migration. The specific signal transduction pathway which becomes activated is dependent on both the cell type and the context in which it takes place. The extreme amino terminus of the chemokine structure is the critical domain for receptor interaction and activation, with subtle changes in this domain able to cause dramatic changes in bioactivity [159].

Table 1.4. Chemokine Ligands and Their Receptors [156]

New name	Original name(s) - Human	Receptor(s)
CXCL1	GROα, MGSA-α	CXCR2 > CXCR1
CXCL2	GROβ , MGSA-β	CXCR2
CXCL3	GROγ, MGSA-γ	CXCR2
CXCL4	PF-4	Unknown
CXCL5	ENA-78	CXCR2
CXCL6	GCP-2	CXCR1, CXCR2
CXCL7	NAP-2	CXCR1, CXCR2
CXCL8	IL-8	CXCR1, CXCR2
CXCL9	MIG	CXCR3
CXCL10	IP-10	CXCR3
CXCL11	I-TAC	CXCR3, CXCR7
CXCL12	**SDF-1**	**CXCR4, CXCR7**
CXCL13	BCA-1, BLC	CXCR5
CXCL14	BRAK, bolekine	Unknown
CXCL15	Unknown	Unknown
CXCL16	SR-PSOX	Unknown
CCL1	I-309	CCR8
CCL2	MCP-1, MCAF	CCR2
CCL3	MIP-1α, LD78α	CCR1, CCR5
CCL4	MIP-1β	CCR5
CCL5	RANTES	CCR1, CCR3, CCR5
CCL6	Unknown	CCR1, CCR2, CCR3
CCL7	MCP-3	CCR1, CCR2, CCR3
CCL8	MCP-2	CCR2, CCR3, CCR5
CCL9/10	Unknown	Unknown
CCL11	Eotaxin	CCR3
CCL12	Unknown	CCR2
CCL13	MCP-4	CCR1, CCR2, CCR3
CCL14	HCC-1	CCR1
CCL15	HCC-2, Lkn-1	CCR1, CCR3
CCL16	HCC-4, LEC	CCR1
CCL17	TARC	CCR4
CCL18	PARC, DC-CK-1	Unknown
CCL19	MIP-3β, ELC, exodus-3	CCR7
CCL20	MIP-3α, LARC, exodus-1	CCR6
CCL21	SLC, exodus-2	CCR7
CCL22	MDC, STCP-1	CCR4
CCL23	MPIF-1	CCR1
CCL24	MPIF-2, Eotaxin-2	CCR3
CCL25	TECK	CCR9
CCL26	Eotaxin-3	CCR3
CCL27	CTAK, ILC	CCR10, CCR2, CCR3
CCL28	MEC	CCR10, CCR3
XCL1	Lymphotactin-α, ATAC, SCM-1α	XCR1
XCL2	Lymphotactin-β, SCM-1β	XCR1
CX3CL1	Fractaline	CX3CR1

1.4.1 The Role of Chemokines in Multiple Myeloma

The homing of antibody-producing PCs to the BM is dependent upon the coordinated expression of integrins (eg. very late antigen (VLA)-4 and VLA-5) and chemokines [163,164]. As B-cells differentiate into PCs within the germinal centre of the spleen and lymph nodes, they undergo a coordinated change in chemokine receptor expression. This involves a loss of responsiveness to the B- and T-cell chemokines CXCL13, CCL19 and CCL21 expressed in the spleen and lymph nodes, and a heightened sensitivity to the effects of CXCL12, which is expressed at high levels in the BM [163,165]. Upon arrival in the BM, malignant PCs home to, and reside in discrete BMSC "niches", which provide a rich source of ECM proteins, adhesion molecules and growth factors critical for the growth and survival of PCs [36].

Primary human MM PCs express several chemokine receptors (eg. CXCR4, CXCR6, CCR1, CCR2, CCR3 and CCR10) and MM cell lines have been shown to express high levels of CXCR3, CXCR4, CCR1, CCR2, CCR5 and CCR6 [166-169]. In addition to expressing and secreting chemokines themselves, MM PCs are influenced by chemokines secreted by other cells within the BM microenvironment such as BMSCs and ECs. Recent studies suggest that the CXCL12-CXCR4 chemokine-receptor pair plays a particularly significant role in MM biology.

1.4.2 CXCL12 and Its Receptor, CXCR4

CXCL12, also known as stromal-derived factor-1 (SDF-1) and pre-B cell growth-stimulating factor, is constitutively expressed throughout the body and exerts a broad range of actions. CXCL12 is highly conserved across phylogenetic boundaries, with 99% homology between the mouse and human sequence [170]. To date, six CXCL12 isoforms, which arise from alternative gene splicing, have been identified in humans: CXCL12α, CXCL12β, CXCL12γ, CXCL12δ, CXCL12ε and CXCL12ϕ [171]. While all of these isoforms exhibit chemotactic activity *in vitro*, they display different tissue distribution patterns, the biological significance of which is yet to be determined. CXCL12α and CXCL12β are the most widely-expressed isoforms and the most characterised [171].

CXCL12 binds to the chemokine receptor, CXCR4. Like all chemokine receptors, CXCR4 is a heptahelical transmembrane receptor that signals through G-proteins, and is regulated by phosphorylation and subsequent internalisation [158]. Originally identified as a co-

receptor for the entry of T-tropic (X4) HIV into $CD4^+$ T cells [172,173], CXCR4 is highly conserved between species, with 94% homology between human and mouse [170]. Like its ligand, CXCR4 is widely expressed throughout the body, particularly the brain, stomach, intestines, kidney and lymphoid organs. CXCR4 is expressed on the majority of leukocytes, as well as on dendritic cells [174-176], ECs [10,12,14,177,178], neurons [179], glial cells [180,181], OCs and OC precursors [9,182,183], epithelial cells [184-186] and megakaryocytes [187-189].

Given the broad expression profiles of both CXCL12 and CXCR4, it is not surprising that multiple functions for this ligand/receptor pair have been identified. Abundantly expressed in the BM, CXCL12 is crucial for the engraftment and retention of stem cells [190,191], the retention of myeloid progenitors [192], the growth of B-cell progenitors [193], the migration of B-cells to secondary lymphoid organs [194] and T-cell development [195]. CXCL12 is also a survival factor for myeloid progenitors [196], neuronal axons [197], placental trophoblasts [198], BMSCs [199], and OCs [200], and is a potent chemotactic factor for monocytes [201], dendritic cells [202], megakaryocytes [189], ECs [10,177,178,203], T-cells [204], leukocytes [201,202], neuronal cells [205] and OC precursors [183,200,206].

Until recently, interactions between CXCL12 and the CXCR4 receptor were believed to be monogamous. This was largely based on the fact that CXCL12 and CXCR4 knockout mice display an identical, lethal phenotype, characterised by deficient lymphopoiesis and myelopoiesis, and abnormal neuronal and cardiovascular development [173,207,208]. However, it is now known that in addition to CXCR4, CXCL12 also binds to the newly de-orphanised receptor, CXCR7 (also known as RDC1, CCX-CKR2 and Cmkor1) [209-211]. To date, the functional significance of CXCR7 is unknown, but it has been shown to be expressed by human memory B-cells, a restricted subset of leukocytes and NK cells, ECs, cardiac microvessels and tumour vasculature [209-212]. At this stage, CXCR7 does not appear to be a classical chemokine receptor, because binding of CXCL12 to CXCR7 does not induce the typical chemokine-induced signalling cascades or chemotaxis [210,211]. Instead, the binding of CXCL12 to CXCR7 induces the heterodimerisation of CXCR4 and CXCR7, which in turn enhances CXCL12-induced signalling through CXCR4 [211].

While little is known of the post-translational regulation of CXCL12, a number of proteolytic enzymes cleave and degrade CXCL12 at the N-terminus, including MMPs, CD26/dipeptidyl peptidase IV, serine proteases and leukocyte elastase [213-215]. The *in vivo*

half-life of CXCL12 is unknown, but is believed to be long-lived when bound to glycosaminoglycans [216].

1.4.3 The Role of CXCL12 in Cancer

High tumour levels of CXCL12 were first observed in ovarian cancer in 2001 [217,218]. Since then, aberrant CXCL12 expression has been found in breast cancer [219], pancreatic cancer [203], thyroid cancer [220], prostate cancer [221], glioblastoma [13,222], and gastric cancer [223].

In 2001, a pivotal study by Muller and colleagues demonstrated that the CXCL12/CXCR4 axis promotes organ-specific tumour metastasis in mammary carcinoma [224]. They showed that CXCR4 is over-expressed in mammary carcinoma cells and that preferential sites of metastasis such as the liver, lymph nodes, adrenal glands, BM and lungs display high levels of CXCL12 expression. Subsequent studies have confirmed that aberrant CXCR4 expression is associated with cancers of the breast [225], prostate [226,227], ovary [228], pancreas [203,229], oesophagus [230,231], lung [232], kidney [233], thyroid [220,234] and bladder [235], as well as osteosarcoma [236], B-cell CLL [237], and ALL [238]. Such widespread expression of CXCR4 in malignant tissues is compelling evidence for the importance of CXCL12 and CXCR4 in tumorigenesis, however the full gamut of tumour-promoting functions of this chemokine pair is yet to be fully elucidated.

Following Muller *et al*'s study, CXCL12 and CXCR4 has been shown to mediate metastasis in lung cancer [232], colorectal cancer [239], hepatocellular carcinoma [240], prostate cancer [227], bladder cancer [235], pancreatic cancer [229], and osteosarcoma [236]. Furthermore, the CXCL12/CXCR4 axis has also been implicated in tumour cell proliferation in gliomas [241], breast cancer [242], lung cancer [232], glioblastoma [222,243], pancreatic cancer [229] and prostate cancer [221], via activation of the ERK signalling pathway [217,226,229,244]. CXCL12 also modulates the expression and function of cell surface integrins to promote tumour cell adhesion [245,246], and has been shown to promote tumour angiogenesis in ovarian cancer [247], breast cancer [242], and glioblastoma [13].

1.4.4 The Role of CXCL12 in Angiogenesis

It was once thought that the presence or absence of a three amino acid motif (Glu-Leu-Arg: the "ELR motif") preceding the first cysteine residue of CXC chemokines determined whether they promote or inhibit angiogenesis, respectively [248]. However, despite an absence of the ELR motif, it widely accepted that CXCL12 is a pro-angiogenic chemokine [10,177,249].

The first indication of a role for CXCL12 and CXCR4 in angiogenesis followed the observation that CXCL12 and CXCR4 knockout mice exhibit defective gastrointestinal vascularisation [208]. Subsequent studies have showed that CXCL12 is expressed by ECs [12,250], and that CXCR4 is the predominant CXC chemokine receptor expressed by these cells [177,178,251,252]. The CXCL12/CXCR4 axis is crucial for many aspects of angiogenesis [253] and elicits a variety of EC responses, including receptor internalisation and calcium fluxes [10,177,249], *in vitro* endothelial tube formation [10], EC branching [12] and EC chemotaxis [10,177,178,203]. In addition to their own direct effects on ECs, angiogenic factors such as VEGF and bFGF also increase CXCL12 and/or CXCR4 expression in human ECs and thereby potentiate the angiogenic actions of CXCL12 [10,12,14,254]. Conversely, the binding of CXCL12 to EC-expressed CXCR4 also enhances the production of VEGF [14,255].

A number of studies have demonstrated that CXCL12 induces *in vivo* angiogenesis via direct subcutaneous injection of rhCXCL12 [10], subcutaneous injection of rhCXCL12 in Matrigel plugs [256-258], and injection of rhCXCL12 into rabbit corneal micropockets [14]. Furthermore, CXCL12 neutralising antibodies have been shown to reduce pathological angiogenesis in an ischaemic eye model of proliferative diabetic retinopathy [259]. The contribution of CXCL12 to tumour angiogenesis remains unclear, as contradictory findings are reported in the literature. In an immunohistochemical study of glioblastoma specimens, tumour expression of CXCL12 and CXCR4 were found to localise to areas of angiogenesis and in tumour cells immediately adjacent to areas of necrosis [13]. Subsequent studies have demonstrated that CXCL12 promotes tumour angiogenesis in ovarian cancer [247], and breast cancer [242]. However in contrast, in a subcutaneous mouse model of non-small cell lung carcinoma, the administration of a CXCL12 neutralising antibody had no effect on tumour MVD, and tumour homogenates from these mice failed to induce angiogenesis in the corneal micropocket system [232]. Similarly, in the 5T33MM murine model of MM, the

administration of a CXCR4 antagonist was found to have no effect on BM MVD [260]. Further studies are required to clarify these contradictory findings.

1.4.5 The Role of CXCL12 in Multiple Myeloma

Although the effects of CXCL12 on normal haemopoietic cells have been investigated, its role in haematological malignancies such as MM is yet to be clearly defined. The significance of the CXCL12/CXCR4 axis in MM is indicated by the fact that CXCR4 is the most represented chemokine receptor on MM PCs [261,262]. Furthermore, CXCL12 is highly expressed by MM PCs [9], and circulating levels of CXCL12 are elevated in the peripheral blood (PB) circulation of MM patients compared to age-matched normal donors and patients with MGUS [9]. CXCL12 is also elevated in the BM of MM patients compared to healthy individuals [263].

CXCL12 plays a role in several aspects of MM biology. One of the very first steps in the homing of MM PCs to the BM is transendothelial migration. CXCL12 promotes this process by up-regulating MMP-9 secretion to facilitate invasion across EC basement membranes [264], and transiently up-regulating MM PC expression of VLA-4 and VCAM-1 integrins to facilitate adhesion to BM endothelium [164,265]. Upon arrival in the BM compartment, interactions between MM PC-expressed CXCR4 and BMSC-derived CXCL12 are critical for MM PC migration and retention within the BM, in close proximity to stromal cells [168,192,266,267]. This is exemplified by recent studies by Menu *et al*, who showed that blockade of the CXCL12/CXCR4 axis induces MM PC mobilisation from the BM in the 5T33MM mouse model [260]. Furthermore, when labelled MM PCs were systemically injected into mice in the presence or absence of a CXCR4 antagonist, a 20% reduction in BM tumour burden was observed [260]. *In vitro* studies have also indicated that CXCL12 mediates partial protection of MM PCs from dexamethasone-induced apoptosis via activation of the Akt survival pathway [268].

CXCL12 is an important chemoattractant for the recruitment of circulating OC precursors to the bone [206], and regulates osteoclastic bone resorption in rheumatoid arthritis [182]. Circulating levels of CXCL12 correlate with the presence of radiologically-detectable osteolytic bone lesions in MM patients [9], suggesting that CXCL12 plays a functional role in mediating osteolysis in MM. This is supported by the observation that CXCL12 increases the number of resorption lacunae and the extent of OC-mediated resorption *in*

vitro [9]. Taken together, these findings suggest that CXCL12 and CXCR4 are promising therapeutic targets in MM.

1.5 Hypoxia

Oxygen homeostasis is governed by a precarious balance between the necessity of oxygen for ATP generation via oxidative phosphorylation, and the risk of oxidative damage to cellular lipids, nucleic acids and proteins caused by excessive oxygen concentrations [269]. When this oxygen homeostasis becomes dysregulated and cells or tissues are deprived of sufficient oxygen, a state of hypoxia is created [270]. Hypoxia is associated with a number of both short- and long-term pathologies such as inflammation and cardiovascular disease [271], and also has special relevance in cancer biology. Due to the fundamental importance of oxygen for cellular metabolism and survival, cells have evolved intricate response mechanisms to detect and respond to changes in local oxygen tensions [272]. These mechanisms involve the activation of cell- and tissue-specific transcription programs that coordinate the expression of hundreds of gene products which mediate a variety of short- and long-term adaptive responses such as erythropoiesis, angiogenesis, vascular remodelling, increased iron transport, cell proliferation and a switch to glycolytic metabolism [272-276].

The mechanisms which mediate these responses are believed to be evolutionarily conserved in all mammalian cells [272]. However, due to differences in energy requirements between different cell types and their residence in distinct microenvironments containing different oxygen levels, not all cells respond to hypoxia in exactly the same manner or to the same degree [277]. Cells also differ in their sensitivity to hypoxia: some cells can survive indefinitely in low oxygen environments, whereas others die within minutes [277]. A number of transcription factors mediate cellular adaptation to hypoxia, including HIF-1 [278], HIF-2 [279], ETS-1 [280], CREB [281], AP-1 [282-284], and NFκB [285]. Of these, the most important regulators of cellular responses to hypoxia are the hypoxia-inducible transcription factors (HIFs).

1.5.1 The Hypoxia-Inducible Transcription Factors

The HIF system operates in virtually all eukaryotic cells and directly and/or indirectly regulates hundreds of genes involved in adaptive cellular responses including erythropoiesis, glycolysis, and angiogenesis [272-276]. The most characterised HIF

transcription factor is HIF-1, which was initially identified during investigations into the oxygen-dependent regulation of erythropoietin production [286]. HIF-1 is a master regulator of oxygen homeostasis and plays a vital role in both embryonic development and postnatal physiology [269]. HIF-1 is a heterodimeric complex composed of an inducible α-subunit, HIF-1α, and a constitutively-expressed β-subunit, aryl hydrocarbon nuclear translocator (ARNT, also termed HIF-1β) [279,286-288].

The HIF-1α protein contains several key structural features, including a basic helix-loop-helix (bHLH) domain, which is responsible for DNA binding and the dimerisation of HIF subunits, and a PAS domain (Per-ARNT-Sim, the first three proteins in which this domain was identified), which forms a secondary dimerisation interface between family members and confers target gene specificity [269]. The oxygen-dependent degradation (ODD) domain, located between residues 401-603, confers normoxic protein instability when specific residues within the domain are hydroxylated [273,289,290]. HIF-1α also contains two transactivation domains (TADs), to which transcriptional co-activators such as CBP/p300 bind. To date, two additional human HIF-1α splice variants have been identified: the first lacks exon 14 but retains the ability to modulate gene expression under hypoxic conditions [291], and the second lacks exons 11 and 12 and appears to be a dominant negative isoform [292] (Figure 1.6).

Homology searches and screens for other ARNT binding partners have led to the discovery of two additional proteins which are structurally and functionally related to HIF-1α (Figure 1.6). The closely-related HIF-2α (also known as endothelial PAS-1 [EPAS-1], HIF-like factor [HLF], HIF-related factor [HRF], and member of PAS superfamily-2 [MOP-2]) shares 48% sequence homology with HIF-1α [293,294] and like HIF-1α, contains a bHLH domain, PAS domain, ODD domain and two transactivation domains. HIF-2α is also stabilised under hypoxic conditions and forms a heterodimeric transcription complex with ARNT, known as HIF-2. However, unlike the ubiquitously-expressed HIF-1α, HIF-2α is selectively expressed in the lung, endothelium, kidney, liver and carotid body and some human cancer cells [293-298].

Both HIF-1 and HIF-2 bind to the same DNA consensus sequence 5'-RCGTG-3' in hypoxia response elements (HREs) located in target gene promoters [293,299]. However, despite the high protein sequence homology and similar oxygen-dependent mechanisms of

Figure 1.6. The Domain Structure of the Human HIF Transcription Factor Subunits. The HIF-1, HIF-2 and HIF-3 transcription factors are heterodimers composed of an inducible α-subunit and a constitutively-expressed β-subunit, known as ARNT. HIF-1α, HIF-2α, HIF-3α, and their respective splice variants, contain various combinations of key protein domains: a bHLH domain, which is responsible for DNA binding and subunit dimerisation; a PAS domain (composed of PAS-A and PAS-B), which forms a secondary dimerisation interface and confers target gene specificity; a carboxy- and/or amino-terminal transactivation domain (C-TAD and N-TAD), to which transcriptional co-activators bind to form the active transcription complex; an inhibitory domain (ID), which negatively regulates TAD activity; and an oxygen-dependent degradation (ODD) domain, which mediates oxygen-dependent protein stability. The constitutively-expressed ARNT contains the bHLH, PAS and C-TAD regions, but lacks the N-TAD, ODD and ID regions.

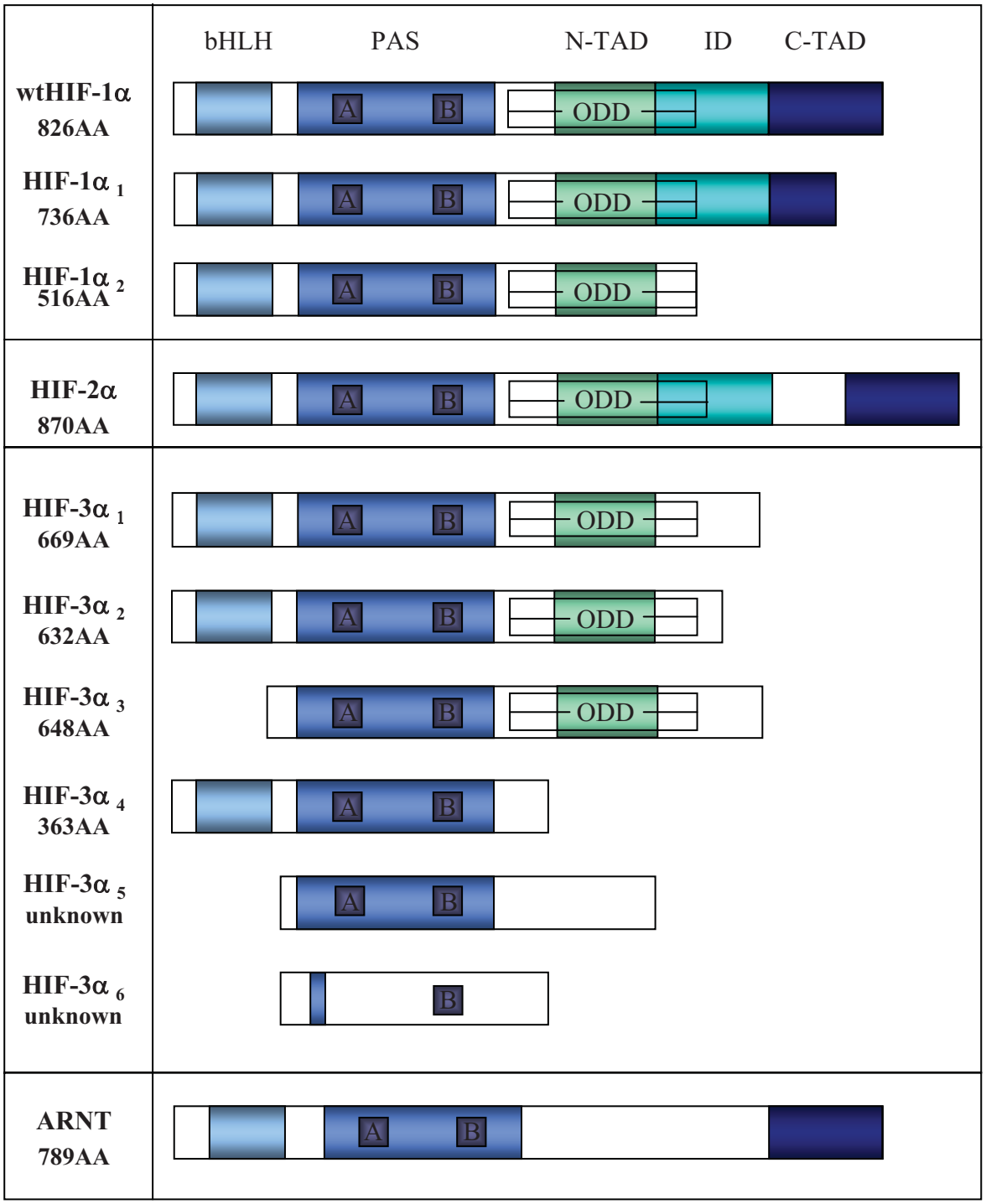
bHLH
PAS
N-TAD
ID
C-TAD
wtHIF-1α
826AA
HIF-1α 1
736AA
HIF-1α 2
516AA
HIF-2α
870AA
HIF-3α 1
669AA
HIF-3α 2
632AA
HIF-3α 3
648AA
HIF-3α 4
363AA
HIF-3α 5
unknown
HIF-3α 6
unknown
ARNT
789AA
A
B
ODD

action between HIF-1α and HIF-2α there are a growing number of subtle physiological and mechanistic differences which indicate distinct, non-redundant roles. For example, while HIF-1 and HIF-2 exhibit overlapping but distinct target gene specificities [300,301], knockout studies have showed that the inactivation of either isoform results in a distinctly different phenotype. HIF-1α$^{-/-}$ mice die during embryogenesis at day E11 due to cardio-vascular malformations, a lack of neural tube closure and defective vascularisation [302,303]. In these mice, the formation of large vessels was unaffected by HIF-1α knockdown, but capillary vessel formation was defective and cephalic vascularisation almost completely absent. These studies indicate a role for HIF-1α in the formation of functional vessels to support expanding tissues. HIF-1α$^{+/-}$ mice develop normally, but exhibit impaired responses to prolonged hypoxia such as pulmonary hypertension, ventricular hypertrophy and aberrant vascular remodelling [304,305].

There is conflicting data regarding the phenotype of HIF-2α knockout mice, which has been attributed to the use of difference mouse strains. In one study, HIF-2α$^{-/-}$ mice developed a normal circulatory system, but died at embryonic day E16.5 due to a de-regulated heartbeat and cardiac failure [296]. In a subsequent study, HIF-2α$^{-/-}$ mice died at embryonic day E12.5, and displayed defects in blood vessel fusion and remodelling [306]. HIF-2α$^{-/-}$ has also been associated with impaired lung maturation, retinal angiogenesis, haemopoiesis and autonomic nervous system development [296,307-309].

Adding complexity to the HIF system is the existence of a third, more distantly related HIF-α gene which has been called HIF-3α [310]. The role of HIF-3α in hypoxia-mediated transcription is unknown but, like HIF-1α and HIF-2α, its activity is up-regulated under hypoxic conditions and it is able to dimerise with ARNT. To date, six splice variants of HIF-3α have been identified (Figure 1.6), and at least one of these isoforms (HIF-3α2, also known as IPAS-1) appears to suppress the activation of hypoxia-inducible gene expression and negatively regulate hypoxia-induced transcription [310].

Thus far, over one hundred hypoxia-responsive HIF target genes have been identified which encode proteins involved with functionally diverse responses such as angiogenesis, erythropoiesis, glucose transport, glycolysis, iron transport, cell proliferation and survival, and vascular remodelling [272-275].

1.5.2 Regulation of the HIF Transcription Factors

Under normal circumstances, the stability and transactivation of HIF-1 and HIF-2 are tightly controlled because they are only required to initiate cell-specific transcription programs when hypoxic conditions are encountered. The HIF system is regulated through the activity and abundance of the HIF-α subunits, and is mediated post-translationally through increased protein stability [311-315]. As summarised in Figure 1.7, the regulation of HIF-1α and HIF-2α protein expression is controlled by a family of three prolyl hydroxylase domain (PHD) proteins which, under normoxic oxygen concentrations, hydroxylate two specific proline residues within the ODD domain [316-320]. This modification facilitates the binding of the von Hippel-Lindau (VHL) tumour suppressor protein, which is a component of a E3 ubiquitin ligase complex that poly-ubiquitinates the HIF-α protein and targets it for rapid proteasomal degradation [312,321,322]. The absolute requirement of oxygen for PHD activity serves as the primary cellular oxygen sensor in this process. When oxygen levels fall, the activity of PHD enzymes is inhibited and levels of HIF-α protein rapidly accumulate. The HIF-α protein then translocates to the nucleus and dimerises with the constitutively-expressed β-subunit, ARNT. Following the recruitment of additional transcriptional co-activators, the active HIF complex mediates the transcription of genes required for adaptive cellular responses to hypoxia [275,289,323-326].

The oxygen-dependent control of HIF protein is mediated by PHD enzymes, the activity of which is induced and inhibited extremely rapidly in response to local oxygen concentrations. Upon exposure to hypoxic conditions, increased protein expression of HIF-1α is detectable within 30 minutes, and peaks between four to eight hours of continuous exposure to hypoxia [327]. In contrast, the expression kinetics of HIF-2α upon exposure to hypoxic conditions differs significantly to that of HIF-1α, with delayed induction observed in response to prolonged exposure (eg. at least 16 hours) to hypoxia [327,328]. Upon re-exposure to oxygen, both HIF-1α and HIF-2α are rapidly degraded and have a half life of less than five minutes [278,286,329].

Other post-translational modifications also regulate HIF activity, with hydroxylation, ubiquitination, acetylation and phosphorylation of HIF-α subunits shown to affect the stability and/or transcriptional activity of these proteins [330]. Under normoxic oxygen tensions, asparaginyl hydroxylation of specific residues within the C-TAD domain regulates HIF activity by blocking the recruitment of transcriptional co-activators such as

Figure 1.7. The Oxygen-Dependent Regulation of the HIF-α Subunit. Under normal oxygen conditions, specific proline and asparagine residues in the HIF-α proteins undergo hydroxylation. Prolyl hydroxylation facilitates the binding of the pVHL tumour suppressor protein, which recruits an E3 ubiquitin ligase complex and leads to the subsequent proteasomal degradation of the HIF-α protein. Asparaginyl hydroxylation prevents transcriptional co-activators from binding to HIF-α, thus rendering it transcriptionally inactive. Under hypoxic conditions, the activity of the prolyl and asparaginyl hydroxylases is inhibited, which prevents the VHL-mediated degradation of HIF-α protein and facilitates the binding of transcriptional co-activators. The stabilised HIF-α subunit dimerises with the constitutively-expressed ARNT subunit to form the active transcription complex, which then translocates to the nucleus and binds to the promoters of target genes to co-ordinate adaptive responses to the hostile hypoxic environment.

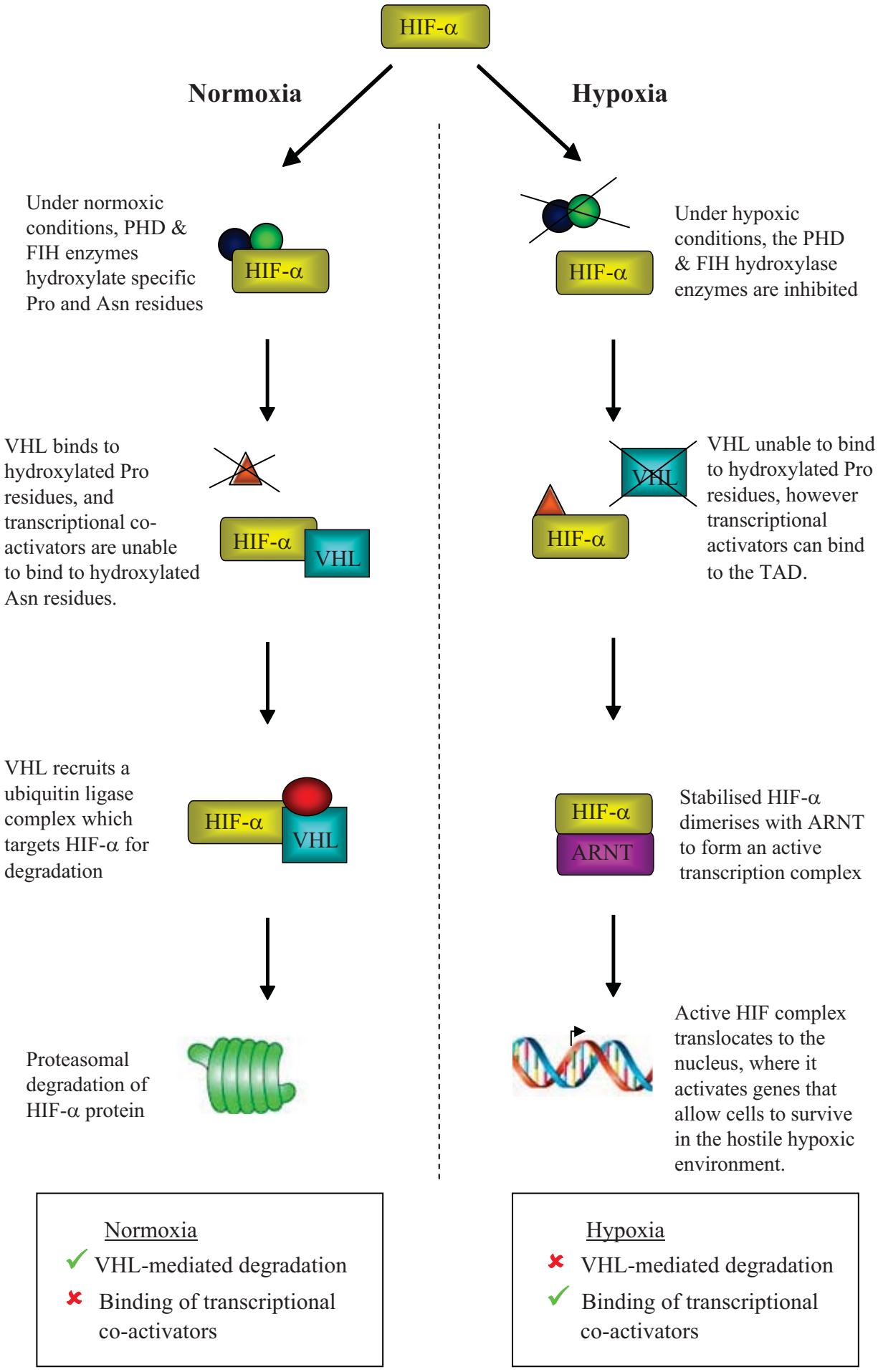
HIF-α
Normoxia
Hypoxia
Under normoxic conditions, PHD & FIH enzymes hydroxylate specific Pro and Asn residues
HIF-α
HIF-α
Under hypoxic conditions, the PHD & FIH hydroxylase enzymes are inhibited
VHL binds to hydroxylated Pro residues, and transcriptional co-activators are unable to bind to hydroxylated Asn residues.
HIF-α
VHL
VHL
HIF-α
VHL unable to bind to hydroxylated Pro residues, however transcriptional activators can bind to the TAD.
VHL recruits a ubiquitin ligase complex which targets HIF-α for degradation
HIF-α
VHL
HIF-α
ARNT
Stabilised HIF-α dimerises with ARNT to form an active transcription complex
Proteasomal degradation of HIF-α protein
Active HIF complex translocates to the nucleus, where it activates genes that allow cells to survive in the hostile hypoxic environment.
Normoxia
✓ VHL-mediated degradation
✗ Binding of transcriptional co-activators
Hypoxia
✗ VHL-mediated degradation
✓ Binding of transcriptional co-activators

CBP/p300 and preventing the formation of the active transcription complex [331]. Acetylation of lysine residues within the ODD domain of HIF-1α by the ARD1 acetyltransferase has also been reported to favour interaction with pVHL and thus promote protein destabilisation [332]. Direct phosphorylation of residues within the C-TAD domain of HIF-1α by MAPK and p38 kinase has been shown to occur after HIF-1α protein stabilisation under hypoxic conditions [325,333]. This modification increases the transcriptional activity of HIF-1 by enhancing its interaction with ARNT [334]. SUMOylation, the covalent binding of Small Ubiquitin-like MOdifiers to a protein, is a more recently reported modifier of HIF. SUMO is a relatively small (12kDa) polypeptide which can bind to HIF-1α and ARNT and negatively regulate transcription [335-337]. While HIF-2α contains two consensus sequences for SUMO, the SUMOylation of HIF-2α has not been shown [330].

In addition to the stabilisation and activation of HIF-α protein under hypoxic conditions, HIF-1α and HIF-2α levels can be aberrantly elevated by genetic alterations and signalling malfunctions which lead to enhanced translation or stability. These events include the loss of tumour suppressor proteins such as VHL [338], p53 [339] and PTEN [340], or the aberrant activation of PI3K/Akt or Src signalling pathways [15,341]. In addition, growth factors and hormones which maintain oxygen homeostasis in normal tissues can also increase HIF-α protein levels under normoxic conditions. These growth factors and hormones include insulin-like growth factor (IGF)-1 [342], IGF-2 [342], angiotensin II [343], thrombin [343,344], PDGF [343,344], IL-1β [345], TNFα [345], and TGFβ [344]. In contrast to hypoxia-mediated protein stability, these growth factors and hormones increase HIF-α protein levels by inducing protein translation [346].

1.5.3 The Role of Hypoxia in Cancer

Hypoxia is an important selective force in the clonal evolution of tumour cells [347]. Using oxygen electrodes to study tumour oxygen supply, Vaupel and colleagues have detected hypoxia in solid tumours [270,348]. Elevated expression levels of HIF have been observed in early stages of tumour development before histological evidence of angiogenesis and invasion, and this is thought to contribute to the angiogenic switch [349]. Increased HIF-1α and HIF-2α expression is a key clinical feature of a number of human malignancies, including cancers of the brain, colon, lung, breast, prostate, kidney, pancreas, cervix, bladder, and ovary [295,349-353]. In these tumours, HIF over-expression arises from both the

hypoxic nature of the tumours and aberrant HIF-1α activation induced by oncogenes. HIF over-expression denotes a highly aggressive disease phenotype and is associated with poor prognosis and resistance to treatment in many cancers, including non-small cell lung carcinoma [354], oligodendroglioma [355], breast carcinoma [356], transitional cell carcinoma of the upper urinary tract [357], pancreatic cancer [358], bladder cancer [359] and osteosarcoma [360]. However, it is important to note that not all HIF target genes favour cell survival. In some cases, HIF activation activates pro-apoptotic genes such as NIP3 [361,362] and RTP801 [363] and mediates cell cycle arrest. This might explain why, in some experimental studies, inactivation of HIF has been shown to favour tumour growth [364,365].

To date, the effect of hypoxia on MM PC survival and proliferation has not been investigated. Unlike other organs, the normal BM microenvironment is physiologically hypoxic, which is crucial for the support of normal BM haemopoiesis [366,367]. Therefore, unlike most other malignancies, MM PCs must survive and grow in an environment which is naturally hypoxic. Recent studies using a murine MM model suggest that during MM disease progression, changes in oxygen levels within the BM microenvironment support the survival and expansion of MM PCs [368].

1.5.4 Hypoxia and Angiogenesis

A tumour's requirement for nutrients and oxygen increases in proportion to its volume, restricting the maximal tumour mass before it experiences nutrient deficiency. It is generally accepted that the limited diffusion distances for oxygen and nutrients between cells restrict the size of solid tumours to 1-2mm in diameter [91], beyond which the innermost tumour cells become hypoxic and necrotic without the recruitment of additional blood supply.

The fundamental link between oxygen levels and angiogenesis was initially proposed following the realisation that VEGF expression was up-regulated by hypoxia [369-371]. Hypoxia is now recognised as a major physical cue for triggering angiogenesis to increase oxygen delivery to oxygen-depleted tissues. Depending on the extent and duration of conditions, hypoxia elicits changes in EC physiology by regulating the synthesis and release of growth factors, cytokines and vasoactive substances, which initiate processes of vascular remodelling required to adapt to low oxygen conditions. As the permeability barrier between circulating blood cells and the underlying vascular tissue, the EC layer of

vascular endothelium is able to respond quickly to circulating factors and environmental stresses, and induces the synthesis of vasoconstricting, vasodilating, mitogenic and remodelling factors [372]. Under hypoxic conditions, HIFs regulate the transcription of genes encoding angiogenic factors such as VEGF [373,374], Ang-2 [375,376], bFGF [377], PDGF [377,378], endothelin-1 [379], TNFα [380], leptin [381,382], and angiogenic receptors such as Flt-1 [383], Tie2 [384,385], and EGFR [386]. The up-regulation of pro-angiogenic proteins locally activates the "angiogenic switch", leading to the induction of angiogenesis.

1.5.5 The Hypoxia-Driven Regulation of CXCL12 and CXCR4

In 2002, Hitchon *et al* demonstrated that CXCL12 expression is up-regulated by hypoxia in cultured human synovial fibroblasts from patients with rheumatoid arthritis and osteoarthritis [387]. This provided the first indication that hypoxia is a regulatory stimulus for CXCL12 expression, however, whilst the authors noted the existence of a candidate HIF consensus binding motif within the CXCL12 promoter, they did not directly examine whether the HIFs mediate the hypoxic up-regulation of CXCL12. Direct evidence of the mechanism by which hypoxia regulates CXCL12 expression was subsequently provided by Ceradini *et al* [15]. Using RNAi technology and chromatin immunoprecipitation, they conclusively showed that HIF-1 binds to the CXCL12 promoter and directly up-regulates CXCL12 expression in HUVECs under hypoxic conditions. The hypoxic induction of CXCL12 expression in areas of ischaemic tissue is thought to attract circulating haemopoietic stem cells to areas of tissue damage [163].

Subsequent studies have demonstrated that hypoxia up-regulates CXCL12 expression in several other cell types, including primary ovarian tumour cells [247], retinal glial cells [388], renal cell carcinomas [389], melanoma cell lines [390], and glioma cell lines [391]. However, one group has also shown that CXCL12 expression is strongly down-regulated by hypoxia in the MCF-7 breast cancer cell line, which suggests that hypoxia-induced changes in CXCL12 expression are cell-specific [392].

Interestingly, expression of the CXCR4 receptor is also up-regulated by hypoxia. In 2003, Staller *et al* [393] reported that CXCR4 expression is negatively regulated by VHL through its degradation of HIF. They associated the mutation of VHL in clear cell renal carcinoma with strong CXCR4 expression and poor survival, thus implicating the hypoxic up-regulation of CXCR4 with tumorigenesis. In the same year, Schioppa *et al* [394] showed that

hypoxia induces a HIF-1-mediated up-regulation of CXCR4 in monocytes, monocyte-derived macrophages, tumour-associated macrophages, ECs, and cancer cells. Subsequent studies have demonstrated hypoxic up-regulation of CXCR4 in HUVECs [395], pancreatic tumour cell lines [229], clear cell renal carcinoma [389], haemangioblastoma [389], renal cell carcinoma [396], glioblastoma [397,398], lymphatic ECs [399], normal and malignant B-cells [400], microglia [401], mesenchymal stem cells [402], and non-small cell lung cancer cells [232,403].

1.6 Summary and Project Aims

MM is an incurable haematological malignancy in which increased BM angiogenesis is associated with a poor prognosis [4-8]. The molecular mechanisms underlying the increased BM angiogenesis in MM are complex and have yet to be fully elucidated. Our present understanding of MM biology indicates that the CXCL12/CXCR4 system plays a particularly important role in several key processes, including transendothelial migration [164,264], MM PC homing to and retention in the BM [168,192,266,267] and osteoclastic bone resorption [9]. While it has been recently reported that CXCL12 is a potent angiogenic factor [10,12,253] and that CXCL12 is aberrantly expressed by MM PCs [9], its role in angiogenesis in MM has not been examined.

Furthermore, the mechanisms by which CXCL12 expression is induced in MM PCs are unknown. Recent studies have shown that CXCL12 expression is up-regulated by hypoxia in a wide range of cell types [15,163,247,387-391], however to date the role of hypoxia on CXCL12 expression in MM PCs has not been examined.

The studies outlined in this thesis were designed to address the following aims:

1. To investigate the role of CXCL12 in the increased angiogenesis in MM using patient-derived peripheral blood and bone trephine specimens and *in vitro* angiogenesis assays.

2. To investigate whether hypoxia and the HIF transcription factors represent a possible mechanism for the aberrant expression of CXCL12 in MM PCs.

3. To develop an *in vivo* mouse model to investigate the role of CXCL12 in the increased angiogenesis in MM.

Chapter 2:

MATERIALS & METHODS

2.1 Suppliers of Commonly Used Reagents

Table 2.1. Commonly Used Reagents and Their Suppliers

Reagent	Supplier	Cat. Number
Acrylamide (30% bis solution)	BioRad Laboratories	161-0158
Anaerogen Hypoxia Sachets	Oxoid	AN0025A
BioRad RCDC Protein Assay	BioRad Laboratories	500-0120
D-Luciferin K^+ (*in vivo* bioluminescence)	Xenogen	XR-1001
Dulbecco's Modified Eagle's Medium, High Modified (DMEM)	SAFC Biosciences	51441C
Endothelial Cell Growth Supplements (ECGS)	Becton Dickinson	BD354006
Foetal Calf Serum (FCS)	MultiSer	15-011-0500V
Gelatin	Sigma	G-9391
Glycogen	Roche	901393
Hanks Balanced Salt Solution (HBSS)	SAFC Biosciences	55021C
Heparin	Sigma	H-4898
HEPES (1M)	SAFC Biosciences	59205C
L-glutamine (200mM)	SAFC Biosciences	59202C
Matrigel (*in vitro*, growth factor-reduced)	BD Biosciences	35-4230
Matrigel (*in vivo,* with growth factors)	BD Biosciences	35-4234
Medium 199/EBSS (M199 with Earle's Balanced Salts)	SAFC Biosciences	51312C
Roswell Park Institute Medium (RPMI-1640)	SAFC Biosciences	51501C
Penicillin G (5000U/mL)-Streptomycin sulphate (5000µg/mL)	CSL Biosciences	05081901
Superscript III	Invitrogen	18080085
Sybr Green	Superarray Bioscience	PA-012
Tris (Sigma-7-9®)	Sigma	T-1378
TRIzol®	Invitrogen	15596-018
Trypan Blue	Sigma	T-8154
Trypsin-EDTA	Gibco	15400-054

2.2 Solutions, Buffers and Media for Cell Culture

2.2.1 Gelatin Solution

Gelatin was required to promote EC adhesion to tissue culture plastic. A gelatin solution consisting of 1.8% (w/v) gelatin was prepared in deionised water heated to 70-80^{o}C, and sterilised by autoclaving at 121^{o}C for 30 minutes on a fluid cycle. Upon cooling, the gelatin solution was supplemented with 2.2% (v/v) 7.5% $NaHCO_3$, 7.5% (v/v) 10x media, and 3.7% (v/v) FCS, which were filter sterilised through a 0.2μm single-use syringe filter (Satorius Minisart, Germany) prior to their addition. The complete gelatin solution was stored at 4^{o}C until required.

2.2.2 HUVEC Medium

Medium 199/EBSS (M199) was supplemented with 20% (v/v) FCS, 20mM HEPES buffer, 100μM non-essential amino acids (Invitrogen, Australia), 60mM sodium pyruvate and 50 i.u./mL penicillin-streptomycin. The medium was subsequently filter-sterilised through a 0.2μm bottle top filter (Nalgene, USA) and stored at 4^{o}C. The medium was replenished with 2mM L-glutamine at weekly intervals.

2.2.3 TrHBMEC Medium

Dulbecco's Modified Eagle Medium (DMEM) was supplemented with 5% (v/v) FCS, 0.1% (w/v) glucose, 10mM HEPES buffer, 2mM L-glutamine and 50 i.u./mL penicillin-streptomycin. The medium was subsequently filter-sterilised through a 0.2μm bottle top filter and stored at 4^{o}C. The medium was replenished with 2mM L-glutamine at weekly intervals.

2.2.4 Roswell Park Memorial Institute Medium (RPMI-1640)-10

Roswell Park Memorial Institute medium (RPMI-1640) was supplemented with 10% (v/v) FCS, 2mM L-Glutamine, 1mM sodium pyruvate, 15mM HEPES buffer and 50 i.u/mL penicillin-streptomycin. The medium was subsequently filter-sterilised through a 0.2μm bottle top filter and stored at 4^{o}C. The medium was replenished with 2mM L-glutamine at weekly intervals.

2.2.5 Dulbecco's Modified Eagle's Medium (DMEM)-10

DMEM was supplemented with 10% (v/v) FCS, 2mM L-Glutamine, 1mM sodium pyruvate, 15mM HEPES buffer and 50 i.u/mL penicillin-streptomycin. The medium was subsequently filter-sterilised through a 0.2μm bottle top filter and stored at 4^{o}C. The medium was replenished with 2mM L-glutamine at weekly intervals.

2.2.6 HHF Wash Buffer

Sterile Hank's Balanced Salt Solution (HBSS) was supplemented with 5% (v/v) sterile FCS, and the resultant wash buffer stored at 4^{o}C.

2.2.7 Blocking Buffer

HBSS was supplemented with 0.4% (w/v) BSA, 4% (v/v) normal human serum (Red Cross, South Australia), 5% (v/v) FCS and 50 i.u./mL penicillin-streptomycin. The final buffer solution was filter-sterilised through a 0.2μm bottle top filter and stored at 4^{o}C.

2.2.8 Flow Cytometry Fixative ("FACS Fix")

Single strength PBS was supplemented with 1% (v/v) formalin, 2% (w/v) D-glucose, and 0.02% (w/v) sodium azide. The fixative was stored at 4^{o}C.

2.2.9 Standard Immunohistochemical Staining Solutions

2.2.9.1 Mayer's Haematoxylin

Deionised water was supplemented with 5% (w/v) aluminium ammonium sulphate, and heated until fully dissolved. Upon cooling, the ammonium sulphate solution was supplemented with 0.5% (w/v) haematoxylin, 1% (v/v) ethanol, 0.1% (w/v) sodium iodate, 2% (v/v) acetic acid and 30% (v/v) glycerol. The complete haematoxylin solution was stored at room temperature (RT).

2.2.9.2 Acid Alcohol (0.3% v/v)

Seventy percent (v/v) ethanol was supplemented with 0.3% (v/v) concentrated HCl and stored at RT. This solution was used to differentiate haematoxylin staining.

2.2.9.3 Scott's Tap Water Substitute

Distilled water was supplemented with 2% $MgSO_4$ and 0.2% $NaHCO_3$, and stored at RT. This solution was used as the blueing agent for haematoxylin staining.

2.3 Cell Culture Techniques

2.3.1 Maintenance of Cell Lines

All appropriate tissue culture techniques were performed in a Class Two Biological Safety Cabinet. All cell lines were maintained in a humidified environment at 37^{o}C in the presence of 5% CO_2. Media were pre-warmed to 37^{o}C prior to use. Where cells were cultured under hypoxic conditions, tissue culture flasks or plates of cells were incubated in a 2L container in the presence of an anaerobic sachet (Oxoid, Australia), double-sealed with parafilm and incubated in a humidified environment at 37^{o}C in the presence of 5% CO_2 for up to 72 hours. The anaerobic sachet was used to create an oxygen-deprived environment containing less than 1% O_2.

2.3.1.1 Human Umbilical Vein Endothelial Cells (HUVECs)

HUVECs were generously provided by Associate Professor Jennifer Gamble (Hanson Institute, Adelaide) and cultured in tissue culture flasks pre-coated with gelatin. Cells were cultured in HUVEC medium supplemented with 15μg/mL of both heparin (Sigma, USA) and ECGS (Becton Dickinson, USA). Every three days, the culture medium was aspirated and replaced with fresh medium supplemented with growth factors and heparin. Confluent monolayers were harvested by rinsing cultures briefly with sterile HBSS, then adding 0.05% (v/v) trypsin-EDTA for 1 minute. Trypsin activity was neutralised with HHF, and detached cells were centrifuged at 400 x g for 5 minutes, washed twice and seeded into fresh gelatin-coated flasks. All experiments were performed using cells from passage 2 - 5.

2.3.1.2 Transformed Human Bone Marrow Endothelial Cell Line (TrHBMEC)

TrHBMECs were generously provided by Dr Babette Weksler (Weill Medical College of Cornell University, New York, USA) and cultured in tissue culture flasks pre-coated with gelatin. After three days in culture, the medium was aspirated and replaced with fresh medium. Confluent monolayers were harvested by trypsinisation and sub-cultured as previously described for HUVECs (Section 2.3.1.1). All experiments were performed using cells from passage 17 - 25.

2.3.1.3 Human Myeloma Cell Lines

Myeloma cell lines RPMI-8226 and U266 were purchased from the American Type Culture Collection. The WL2 cell line was kindly provided by Professor Doug Joshua (Royal Prince Alfred Hospital, Sydney, Australia). The myeloma cell lines JIMI, LP-1,

OPM-2, and NCI-H929 were kindly provided by Associate Professor Andrew Spencer (The Alfred Hospital, Melbourne, Australia). All myeloma cell lines were cultured in RPMI-1640-10, and cultured at a cell density of 2–5 x 10^5 cells/mL (unless otherwise specified), to ensure that the majority of cells were in a logarithmic phase of growth. Cells were subcultured into fresh media every two to three days.

2.3.1.4 HEK-293T Packaging Cell Line

HEK-293T cells were cultured in DMEM-10 medium and cells were subcultured every three days by trypsinisation as described previously (Section 2.3.1.1).

2.3.2 Cryopreservation of Cells

Cells were cryopreserved in FCS containing 10% (v/v) of the cryoprotectant, dimethyl sulphoxide (DMSO). Immediately prior to freezing, 0.5mL of sterile freeze mix (20% (v/v) DMSO in FCS) was added to 0.5mL of FCS containing 5–10 x 10^6 cells. The cell mixture was immediately transferred to cryoampoules (Greiner Labortechnik, Germany) and placed in a "Mr Frosty" freezing container (Nalgene, USA) at -80^{o}C for at least three hours. Cryoampoules were then transferred to liquid nitrogen storage (-196^{o}C).

2.3.3 Thawing of Cryopreserved Samples

Following removal from liquid nitrogen storage, ampoules were rapidly thawed in a 37^{o}C water bath and the cells quickly transferred to a 14mL round-bottom polypropylene tube. 3mL of pre-warmed media was added drop-wise with constant mixing, and then the sample was made up to a final volume of 10mL. Cells were pelleted by centrifugation at 400 x g for 5 minutes and the supernatant discarded. The cells were subsequently washed two times in media to remove residual DMSO before being seeded into a 75cm^2 tissue culture flask with 15mL media. Cells were incubated at 37^{o}C as per specified conditions of culture.

2.3.4 Collection of Conditioned Media

Non-adherent cells were seeded in 40mL of their appropriate media in a T75 tissue culture flask and incubated in a humidified environment at 37^{o}C in the presence of 5% CO_2. When cells achieved the required density (up to 1 x 10^6 cells/mL), the contents of the flask were transferred to a 50mL tube and centrifuged at 400 x g for 5 minutes. The cell pellet was discarded and the supernatant (ie. the conditioned medium, CM) was filtered through a low

protein binding 0.45μm syringe filter (Nalgene, USA), aliquotted and stored at -20°C until required.

2.3.5 Cell Counts and Viability

Cell counts and viabilities were determined using trypan blue dye exclusion, by diluting cells in 0.4% (w/v) trypan blue (Sigma, USA) and enumerating cells using a haemocytometer and a light microscope (Olympus BX40, Japan).

2.3.6 *In vitro* Tube Formation Assays

Frozen aliquots of growth factor-reduced Matrigel were thawed overnight on ice at 4°C and subsequently kept at or below 4°C while not in use to prevent polymerisation. All tips and plasticware were also kept chilled to prevent Matrigel polymerisation. For the required number of treatments, 100μl of Matrigel was pipetted into 6mm diameter tissue culture wells (96-well plate) using pre-chilled pipette tips and left to polymerise at 37°C for 30 minutes. HUVECs, treated with the appropriate factor(s), were plated onto the polymerised Matrigel at a density of 2.5 x 10^4 cells per well in 100μl M199 medium. Each dose of control or test compound was assayed in triplicate. Assays were incubated in a humidified environment at 37°C in the presence of 5% CO_2. After 7 and 21 hours, the cultures were photographed (40x magnification) and the sum total length of all tubes formed in each well was quantitated from digital photographs using the OLYSIA BioReport image analysis software (Olympus Corporation, Japan). Tubes were defined as cellular extensions linking cell masses or branch points.

2.3.7 Cytokines and Inhibitors Used in This Study

Table 2.2. Cytokines and Inhibitors Used In This Study

Cytokine	Source
VEGF	Peprotech, Cat #100-20
bFGF	Peprotech, Cat #100-18B
CXCL12	Peprotech, Cat #300-28A
T140 (anti-CXCR4)	4F-Benzoyl-TE14011, provided by Professor Nobutaka Fujii, Dept of Bioorganic Medicinal Chemistry, Japan

All cytokines were reconstituted according to manufacturer's instructions and diluted to the appropriate concentration in serum-free media or PBS as required and stored at -80°C.

2.3.8 Cell Proliferation Assay (WST-1)

Cells were seeded into 6mm diameter tissue culture wells (96-well plate) at 4 x 10^3 cells per well in 100µl of the appropriate media using preparative cell sorting, and cultured in a humidified environment at 37^{o}C in the presence of 5% CO_2. The relative number of viable cells in each well was determined at days 1, 3, 5 and 7 using the colorimetric assay reagent WST-1 (4-[3-(4-Iodophenyl)-2-(4-nitrophenyl)-2H-5-tetrazolio]-1,3-benzene disulphonate, Roche, USA) according to manufacturers' instructions. Briefly, 10µl of WST-1 was added to each well (and to wells containing medium alone, to enable background subtraction) and incubated for 90 minutes at 37^{o}C. The optical density of the dye solution was measured with a plate reader (Bio-Rad Model 3550, USA) at 450nm wavelength. This assay is based on the enzymatic cleavage of the WST-1 reagent to form a formazan salt. Quantification of the level of formazan salt is directly proportional to the number of viable cells present in each well. All treatments were assayed in quadruplicate.

2.3.9 Immunofluorescent Staining and Flow Cytometric Analysis

Flow cytometry was performed using an Epics®-XL-MCL analyser (Beckman Coulter, USA). Cells to be analysed were immunostained with primary antibodies targeting antigens of interest. Cell populations were analysed on the basis of their forward and side light scattering properties, which are indicative of cell size and cell density, respectively.

2.3.9.1 Single Colour Immunofluorescence Staining

Cells were harvested from culture (1 x 10^5 cells per condition) and pelleted by centrifugation at 400 x g for 5 minutes at 4^{o}C. Cells were resuspended in ice-cold blocking buffer and incubated on ice for 45 minutes. For each condition, cells were incubated with 50µl of the appropriately diluted primary antibody or isotype-matched control (Table 2.3) in HHF buffer on ice for 1 hour. Cells were washed twice in chilled HHF, to remove unbound antibody, and pellets were resuspended in 50µl HHF containing 1:50 dilution of phycoerythrin (PE)-conjugated goat anti-mouse immunoglobulin (Ig) (Southern Biotechnology, USA). Following incubation with secondary antibody on ice for 45 minutes, the cells were washed as above and fixed in "FACS Fix". Typically, for each sample, 5000-10000 events were analysed by flow cytometry, and stored as list mode data for further analysis using WinMDI software (Windows Multiple Document Interface Flow Cytometry Application, version 2.8).

2.3.9.2 Primary Antibodies Used For Flow Cytometric Analysis in This Study

Table 2.3. Primary Antibodies Used For Flow Cytometry Staining

Antibody	Isotype	Source	Catalogue No.
CXCR4	IgG_{2B}	R&D Systems	MAB173
CXCR4	IgG_{2A}	R&D Systems	MAB171
CXCL12	IgG_1	R&D Systems	MAB350
1B5	Purified mouse IgG_1 (isotype-matched negative control)	In house	N/A
1D4.5	Purified mouse IgG_{2A} (isotype-matched negative control)	In house	N/A
1A6.11	Purified mouse IgG_{2B} (isotype-matched negative control)	In house	N/A

All primary antibodies were used at a concentration of 10μg/mL.

2.3.10 Immunohistochemical Staining

2.3.10.1 Bone Marrow Angiogenesis Analysis in Human Trephine Samples

Five micron sections of mercuric chloride-fixed paraffin embedded biopsy specimens (taken from the posterior iliac crest of MM and MGUS patients, and from individuals who underwent BM biopsies, but were subsequently found to be haematologically normal) were used in this study. All studies were carried out with the approval of the Institutional Ethics Review Committee of the University of Adelaide, the Institute of Medical and Veterinary Science and the Royal Adelaide Hospital, following written informed consent. Biopsy sections were immunostained with an EC-reactive monoclonal antibody against CD34 essentially as previously described [4]. The MVD for each patient trephine specimen was determined according to two established protocols: (1) the "hot spot" method, which assesses MVD at three biopsy regions displaying the highest vascularity [6,117,404-406], and (2) by assessing MVD across the entire biopsy specimen, and taking the overall average [8,106,134,407,408]. In both assessments, the number of individually stained microvessels (capillaries and small venules which did not exceed 10μm) were counted at 200x magnification. Areas of staining with no discrete breaks were counted as a single vessel, and the presence of a lumen was not required. The mean number of microvessels was used as a quantitative measure of BM angiogenesis. All MVD assessments were performed in a blinded manner to limit subjectivity.

2.3.10.2 Detection of CXCL12 in Sections of Bone Marrow Trephine

Five micron sections of paraffin-embedded trephine samples were cut onto Snowcoat X-tra slides (Surgipath, USA) and endogenous peroxidase activity neutralised by incubation with 0.5% H_2O_2 (v/v) in methanol for 30 minutes. Microwave antigen retrieval was performed in the presence of 1mM EDTA, pH 8.0 buffer and then allowed to cool to 40^oC, rinsed in distilled water, and non-specific binding blocked by incubating sections with 3% (v/v) normal horse serum in PBS for 1 hour at RT. Slides were then incubated overnight with either an isotype-matched, non-binding control monoclonal antibody (1B5, IgG_1) or the anti-CXCL12 monoclonal antibody (MAB350, R&D Systems, USA) at a concentration of 2μg/mL in 3% (v/v) normal horse serum in PBS. Slides were then washed three times with "wash buffer" (50mM Tris-HCl + 0.1% Tween-20 in deionised water) and bound antibody was revealed using the Dako EnVision+® Kit (Dako, Australia). Briefly, the slides were incubated with the "Peroxidise-Labelled Polymer" for 30 minutes, then washed with "wash buffer" and incubated with the "DAB Substrate-Chromogen" solution for 5-10 minutes. Slides were counterstained briefly with haematoxylin solution and mounted in PIX.

2.3.10.3 Detection of HIF-1α and HIF-2α in Sections of Bone Marrow Trephine

Five micron sections of paraffin-embedded trephine samples were cut onto Snowcoat X-tra slides (Surgipath, USA) and endogenous peroxidase activity neutralised by incubation with 0.5% H_2O_2 (v/v) in methanol for 30 minutes. Microwave antigen retrieval was performed in the presence of 1mM EDTA, pH 8.0 buffer and then allowed to cool to 40^oC, rinsed in distilled water, and non-specific binding blocked by incubating sections with 3% (v/v) normal horse serum in PBS for 1 hour at RT. Slides were then incubated overnight with either an isotype-matched, non-binding control monoclonal antibody, the anti-HIF-1α monoclonal antibody (Becton Dickinson, USA) or the anti-HIF-2α monoclonal antibody (Novus Biologicals, USA) at a concentration of 2μg/mL in 3% (v/v) normal horse serum in PBS. Slides were then washed three times with "wash buffer" (50mM Tris-HCl + 0.1% Tween-20 in deionised water) and bound antibody revealed using the Dako EnVision+® Kit as described in Section 2.3.10.2.

2.3.11 CXCL12 ELISA Immunoassay

The CXCL12 immunoassay was performed using a commercial human CXCL12 ELISA kit (Human SDF-1α Quantikine Colorimetric Sandwich ELISA, R&D Systems, USA) according to the manufacturer's instructions. Briefly, 100µl of "Assay Diluent" and 100µl of CXCL12 standard dilutions or samples (heparinised patient PB plasma or cultured CM) were added to each well and incubated for 2 hours at RT on a horizontal orbital shaker. The plate was washed four times with "Wash Buffer", with complete removal of liquid at each step and 200µl of "SDF-1α Conjugate" was added to each well and incubated for 2 hours at RT on the shaker. The wash step was repeated, and 200µl of "Substrate Solution" was added to each well prior to a 30 minute incubation at RT in the dark. The reaction was terminated by the addition of 50µl "Stop Solution" to each well, and the optical density of each well was measured using a microplate reader (BIO-RAD, Model 3550, USA) set to 450nm, with 540nm as the reference wavelength. The absolute CXCL12 concentration was determined using a standard curve (0-10ng/mL recombinant CXCL12) generated according to the kit's instructions.

2.4 *In vivo* Techniques

2.4.1 Mouse Strain and Animal Care

Strict animal care procedures set forth by the IMVS Institutional Ethics Committee were followed for all *in vivo* experiments described. Mice used in these studies were four- to six-week old BALB/*c nu/nu* mice, purchased from the University of Adelaide Animal Facility (Adelaide, South Australia) and housed at the IMVS Animal Care Facility (Adelaide, South Australia). In each study, animals were randomly assigned to treatment groups.

2.4.2 Intratibial Injection of Myeloma Cells

Cells (1×10^6 per implant) were washed and resuspended in sterile PBS at a concentration of 1×10^8 cells/mL. Mice were anaesthetised by intraperitoneal administration of 80mg/kg Ketamine and 10mg/kg Xylazine in PBS, and placed on a nose-cone to maintain continuous exposure to 3% (v/v) isofluorane anaesthesia throughout surgery. Using a gas-sterilised Hamilton syringe with a 26-gauge needle, 10µl of the cell mixture was injected through the tibial plateau into the left tibia of each mouse. As a negative control measure, an equivalent volume of sterile PBS was injected into the right tibia of each mouse. After four to six weeks, mice were humanely killed, and the left and right femur and tibia carefully removed and processed for paraffin embedding.

2.4.3 Subcutaneous Implantation of Alzet Osmotic Pumps

Prior to pump implantation, mice were anaesthetised by 3% (v/v) isofluorane inhalation and placed on a nose-cone to maintain continuous exposure to anaesthesia throughout surgery. An Alzet micro-osmotic pump (Model 1002, DURECT Corporation, USA) containing approximately 100µl of the CXCR4 antagonist, T140 (4F-benzoyl-TN14003, 80mg/mL in PBS) was subcutaneously implanted in the upper dorsum of each mouse, and the wound closed with wound clips. This model of pump is designed to deliver the drug at a rate of 0.25µl/hour, and lasts for two weeks. In all studies presented in this thesis, Alzet pumps were implanted two days prior to the implantation of MM cells.

2.4.4 Subcutaneous Implantation of Myeloma Cells - Matrigel

Cells (5 x 10^6 per implant) were washed and resuspended in 200µl ice-cold, serum-free RPMI 1640 medium. The cell suspension was then mixed with an equal volume of Matrigel matrix (Becton Dickinson, USA), using pre-cooled pipette tips to avoid polymerisation of the matrix, and the mixture was placed on ice. Mice were anaesthetised by 3% (v/v) isofluorane inhalation and placed on a nose-cone to maintain continuous exposure to anaesthesia throughout surgery. Using pre-cooled syringes and 26-gauge needles, the chilled mixture was subcutaneously injected into the right ventral flank of the anaesthetised mouse and allowed to solidify under a heat lamp. As a negative control, an equivalent implant containing serum-free media and Matrigel but without cells, was also injected subcutaneously into the left ventral flank of each mouse. After 14 days, mice were humanely killed and the Matrigel plugs and the surrounding tissue photographed, removed, and haemoglobin content assessed as outlined in Section 2.4.6.

2.4.5 *In vivo* Bioluminescence Scanning

All of the cells used for *in vivo* experiments were transduced with the SFG-$_{NES}$-TGL luciferase construct, to enable the ongoing assessment of tumour growth by bioluminescence scanning. For *in vivo* bioluminescence imaging, mice were administered the D-luciferin K^+ substrate (Xenogen, USA) by intraperitoneal injection at a concentration of 150mg/kg in sterile PBS. Levels of bioluminescence emitted from implanted tumour cells were detected with the Xenogen IVIS^{TM} system (Xenogen, USA) An initial time course study measuring bioluminescence intensity at 5 minute intervals following the administration of D-luciferin revealed maximal signal intensity at 30 minutes, which remained relatively constant for a period of 30 to 50 minutes. On the basis of this study, all

subsequent bioluminescence data acquisitions were performed 30 minutes after the administration of D-luciferin.

Thirty minutes after administration of D-luciferin, mice were anaesthetised by 3% (v/v) isofluorane inhalation and placed onto a warmed stage inside the light-tight chamber, with continuous exposure to anaesthetic via a nose-cone. Sequential bioluminescence images were recorded by varying the time of exposure and aperture of the camera. Imaging times ranged from 1 second to 1 minute, depending on the number of cells injected and the extent of tumour growth. Using the Living Image 2.50.1® software (Xenogen, USA), levels of bioluminescence were quantified at tumour sites. The highest bioluminescence reading for each mouse was selected from the sequential images taken at each time point. Mice were imaged weekly for the duration of the experiment.

2.4.6 Assessment of Haemoglobin Content in Murine Implants (Drabkin's)

Subcutaneously implants were photographed, harvested and transferred to an eppendorf tube containing 300µl Milli-Q water. Implants were weighed, and sonicated for 15 minutes (30s pulses with 30s rest periods) using a BioRuptor™ waterbath sonicator (Diagenode, Belgium). Debris was removed by centrifugation at 16,000 x g for 90 minutes at 4˚C. Supernatants were transferred to fresh tubes and stored at -20^{o}C.

The Drabkin's haemoglobin assay was performed as per manufacturers' instructions. Briefly, Drabkin's reagent (Sigma, USA) was prepared with Brij-35 Solution (Sigma, USA) as per the manufacturer's instructions. Fifty microlitres per well of tumour supernatants were transferred to a 96-well tray and 200µl/well of Drabkin's solution was added. The plate was incubated for 15 minutes at RT (to allow the colour to develop from the conversion of haemoglobin to haemoglobin ferricyanate) and then read at 540nm on a plate reader (Bio-Rad Model 3550, USA). A standard curve was generated using bovine haemoglobin (Sigma, USA) dissolved in deionised water as per the Drabkin's protocol.

2.4.7 Analysis of Angiogenesis Data from Subcutaneous Implantation of MM PCs

The data from the Drabkin's assessment of haemoglobin content in the subcutaneous cell implants was initially analysed by normalising the haemoglobin content of the cell implant to the haemoglobin content of the corresponding control implant for each mouse. This normalised haemoglobin assessment was subsequently normalised to the Xenogen

bioluminescence reading obtained at the time of sacrifice, in order to relate the angiogenesis assessment to the number of viable cells present in the implant.

2.5 Molecular Biology Buffers and Reagents

2.5.1 Diethyl pyrocarbonate (DEPC)-Treated (RNase-free) Milli-Q Water

Milli-Q water for RNA and cDNA work was treated with 0.1% (v/v) DEPC (Sigma, USA), a potent inhibitor of RNases. The mixture was incubated overnight at RT, and then autoclaved to remove all traces of DEPC that might otherwise modify purine residues in RNA by carboxymethylation.

2.5.2 Luria Broth (L-Broth)

A broth containing 1% (w/v) Bacto-tryptone (Becton Dickinson, USA), 0.5% (w/v) yeast extract (Becton Dickinson, USA), and 1% (w/v) NaCl was prepared in Milli-Q water. The solution was pH adjusted to pH 7.0 with NaOH, and sterilised by autoclaving on a fluid cycle. The broth was stored at RT until required.

2.5.3 LB Agar

1.5% (w/v) Bacto-agar (Becton Dickinson, USA) was dissolved in L-broth, autoclaved on a fluid cycle and cooled with gentle mixing to prevent solidification. Ampicillin (100μg/mL) was added to the LB agar when cool enough to handle, and plates poured into 100mm bacterial-grade petri dishes. LB agar plates were stored at 4^{o}C.

2.5.4 5 x Acrylamide Load Buffer

A buffer comprising 50% sucrose (w/v), 5mM EDTA, 50mM Tris-HCl pH 7.4, 0.1% bromophenol blue (w/v), and 0.1% xylene cyanol (w/v) was prepared in Milli-Q water. The load buffer was stored at RT.

2.5.5 2x Reducing Load Buffer

A buffer comprising 125mM Tris-HCl pH 7.4, 20% glycerol (v/v), 4% SDS (w/v), 0.04% bromophenol blue (w/v) and 10% β-mercaptoethanol (v/v) was prepared in Milli-Q water. Aliquots of the load buffer were stored at -20^{o}C until required for western immunoblotting.

2.5.6 SDS "Running Buffer" for Electrophoresis

A buffer comprising 0.3% (w/v) Tris-HCl, 1.44% (w/v) Glycine, 0.1% (w/v) SDS was prepared in water, then the solution was pH adjusted to pH 8.3 and stored at RT.

2.5.7 SDS-PAGE "Transfer Buffer" for Electrophoresis

A buffer comprising 0.3% (w/v) Tris-HCl, 1.44% (w/v) Glycine, 15% Methanol (v/v), and 0.1% SDS was prepared in water, pH adjusted to pH 8.3 and stored at 4^{o}C. Each batch of transfer buffer was used twice and then discarded.

2.5.8 1x TBE Buffer for Electromobility Shift Assays

A buffer comprising 50mM Tris-HCl, 1mM EDTA, and 42mM Boric Acid was prepared in Milli-Q water, then the solution was pH adjusted to pH 8.3 and stored at RT.

2.6 Molecular Biology Techniques

RNA TECHNIQUES

2.6.1 Preparation of Total Cellular RNA

Total cellular RNA was extracted from 0.3–5 x 10^6 cells using the TRIzol® Method (Invitrogen, Australia). Briefly, cells were washed in PBS, and lysed in 1mL TRIzol® solution. The RNA was extracted by the addition of 1/5 volume of chloroform, mixed with vigorous shaking, and incubated for 3 minutes at RT. Samples were centrifuged at 12,000 x g for 5 minutes at 4^{o}C to separate phases, and the aqueous phase (containing RNA) was carefully removed and transferred to a fresh RNase-free 1.5mL eppendorf tube. Total RNA was precipitated by the addition of 500µl isopropanol and 2µl ribonuclease (RNase)-free glycogen, and incubated on ice for 5 minutes. The RNA was pelleted by centrifugation at 12,000 x g for 15 minutes at 4^{o}C, washed with 75% (v/v) ethanol. The RNA was resuspended in RNase-free DEPC-treated Milli-Q water and heated to 60^{o}C for approximately 10 minutes to facilitate solubilisation of RNA. The RNA was used immediately for cDNA synthesis or stored at -80^{o}C until required.

2.6.2 Determination of RNA Concentration and Purity

The concentration of RNA in solution was determined by measuring the absorption at 260nm on a UV spectrophotometer (Nanodrop-1000, Thermo Fisher Scientific, USA), assuming that an A_{260} of 1.0 represents 40µg/mL of RNA. The purity of the RNA was

determined by the ratio of A_{260}:$A_{280,}$ where a ratio of >1.8 is considered to represent highly pure RNA. The A_{260}:A_{280} were consistently in the range of 1.8-1.95.

2.6.3 Synthesis of Complementary DNA (cDNA)

Total cellular RNA was extracted from cell lines with TRIzol® as described in Section 2.6.1. Total RNA (1-2µg) was reverse transcribed into single-stranded cDNA using Superscript III (Invitrogen, Australia) according to manufacturer's instructions. Briefly, the RNA sample was resuspended in a total volume of 12µl with RNase-free DEPC treated water prior to the addition of 2µl of random hexanucleotide primers (250ng/µl). The solution was incubated at 70°C for 10 minutes and immediately chilled on ice. The heat-denatured RNA was added to 8µl of 5x first strand buffer, 4µl of 0.1M DTT solution, 4µl of 5mM dNTPs and 2µl Superscript III enzyme (Invitrogen, Australia). The reaction mixture was incubated for 10 minutes at 25°C then 50 minutes at 42°C and finally at 70°C for 10 minutes. The cDNA samples were then diluted 1:4 with RNase-free DEPC-treated water and either used immediately for PCR or frozen at –20°C.

2.6.4 Real-Time Polymerase Chain Reaction (PCR)

Real-Time PCR reactions were performed in a Rotor-Gene PCR machine (Corbett Research, Australia) according to the parameters outlined in Figure 2.1. For each reaction, 4µl of cDNA (previously diluted 1:4 with RNase-free DEPC-treated water) was used in a reaction mixture containing 1µl RNase-free DEPC-treated water, 0.5µl forward primer (100ng/µl working stock), 0.5µl reverse primer (100ng/µl working stock) and 5µl Sybr Green Mix (Superarray Bioscience, Australia).

Figure 2.1. Cycling Parameters for Real Time PCR

	50°C - 2 min	
	95°C - 15 min (enzyme activation)	
Cycling	95°C - 15 sec (denaturation) 60°C - 26 sec (primer annealing) 72°C - 10 sec (primer extension)	48-52 cycles
	72°C - 30 sec (final extension)	
Melt cycle	stepwise increase in temp from 72°C to 99°C	

2.6.5 Primers Used in This Study

Table 2.4. Primers Used In This Study (Human)

Target	Accession Number	Sense/Antisense Primer Sequences	Product Size (bp)
GAPDH	NM_002046	ACCCAGAAGACTGTGGATGG/ CAGTGAGCTTCCCGTTCAG	139
β_2M	NM_004048	AGGCTATCCAGCGTACTCCA/ TCAATGTCGGATGGATGAAA	112
CXCL12 ($\alpha\beta$ isoforms)	NM_000609	ATGCCCATGCCGATTCTTCG/ GTCTGTTGTTGTTCTTCAGCC	128
CXCR4	NM_001008540	CAGCAGGTAGCAAAGTGACG/ GTAGATGGTGGGCAGGAAGA	208
HIF-1α	NM_001530	CCACCTATGACCTGCTTGGT/ TGTCCTGTGGTGACTTGTCC	269
HIF-2α	NM_001430	CTCTCCTCAGTTTGCTCTGAAAA/ GTCGCAGGGATGAGTGAAGT	210
GLUT-1	NM_006516	GGCCAAGAGTGTGCTAAAGAA/ CAGCGTTGATGCCAGACA	200
VEGF	NM_003376	ATGCCAAGTGGTCCCAGG/ CACACAGGATGGCTTGAAGA	176
DEC-1	NM_017418	CAGTGGCTATGGAGGAGAATCG/ GCGTCCGTGGTCACTTTTG	129
NDRG-1	NM_006096	ACAACCCCCTCTTCAACTACG/ GGACTCCAGGAAGCATTTCA	159

DNA TECHNIQUES

2.6.6 Preparation of Chemically Competent DH5α Cells

A single colony was inoculated into 10mL L-Broth grown overnight in a 37^{o}C shaking incubator. This starter culture was then used to inoculate 200mL L-Broth and was grown at 37^{o}C, shaking until the culture reached OD_{600} = 0.6. The bacteria were incubated on ice for 30 minutes, then pelleted at 3000 x g, 4^{o}C for 5 minutes. The cells were then resuspended in 25mL ice-cold 0.1M $MgCl_2$ and pelleted again at 3000 x g, 4^{o}C for 5 minutes. Cells were resuspended in 8mL ice-cold 0.1M $CaCl_2$ + 15% glycerol and incubated on ice for 1 hour. Aliquots were frozen and stored at -80^{o}C until required.

2.6.7 Transformation of Competent Cells

For transformation of ligations into competent *E.coli*, 2µl of the ligation reaction (Section 2.6.11) was added to 100µl competent cells, mixed gently and incubated on ice for 30 minutes. The cells were then heat-shocked at 42^{o}C for 2 minutes and then placed back on ice for 5 minutes. After incubation, 200µl SOC medium was added to the cells and incubated for 30 minutes in a 37^{o}C shaking incubator. Of this mixture, 100µl was plated onto L-Agar plates containing 100µg/mL Ampicillin and incubated at 37^{o}C overnight. Transformed colonies were picked and used to inoculate L-broth for subsequent plasmid purification.

2.6.8 Preparation of Glycerol Stocks

Glycerol stock cultures of log phase bacterial cultures were prepared by the dilution of an overnight culture in an equal volume of 80% (v/v) glycerol and stored at -80^{o}C for long term storage.

2.6.9 Purification of Plasmid DNA from Bacterial Cultures

2.6.9.1 Small Scale Plasmid DNA Extraction (Mini-Prep)

Mini-Prep DNA extractions were performed according to manufacturer's instructions using the Qiagen Plasmid Midi-prep kit (Qiagen, USA).

2.6.9.2 Medium Scale Plasmid DNA Extraction (Midi-Prep)

Midi-Prep DNA extractions were performed according to manufacturer's instructions using the Qiagen Plasmid Midi-prep kit (Qiagen, USA).

2.6.10 Manipulation of DNA Products

2.6.10.1 Quantitation of DNA

The concentration of DNA in solution was determined by measuring the absorption at 260nm on a UV spectrophotometer (Nanodrop-1000, Thermo Fisher Scientific, USA), assuming that an A_{260} of 1.0 represents 50µg/mL of DNA (1cm light path).

2.6.10.2 Restriction Digestion of DNA

Restriction digestion of DNA were performed by digesting 1µg of DNA with 10 units of restriction enzyme in the presence of 1x digestion buffer in a total reaction volume of 10µl. The reaction was incubated at 37^{o}C for 1-2 hours.

2.6.11 DNA Ligation

Ligations were routinely carried out in a total volume of 10µl containing DNA insert:vector of 3:1 (molar ratio), 1x ligation buffer (50mM Tris HCl pH 7.8, 10mM $MgCl_2$, 10mM DTT, 1mM ATP) and 2 units of T4 DNA ligase at RT for 2 hours.

2.6.12 Sequencing

Plasmid DNA was isolated and purified as described in 2.6.9.2. Direct sequencing of double-stranded (ds) PCR products was performed using the ABI PRISM^{TM} Ready Reaction DyeDeoxy^{TM} Terminator Cycle Sequencing Kit (Perkin Elmer, USA), according to the manufacturer's instructions. Sequencing reactions were analysed by the Division of Molecular Pathology, Institute of Medical and Veterinary Science (Adelaide, South Australia).

PROTEIN TECHNIQUES

2.6.13 Preparation of Nuclear Extracts

Cells were centrifuged at 400 x g for 5 minutes at 4^{o}C and then washed twice with cold PBS. Whilst on ice, the cells were resuspended in 800µl "Buffer A" (10mM HEPES pH7.8, 10mM KCl, 1.5mM $MgCl_2$, 0.1mM EDTA, 0.1mM EGTA, 1mM PMSF, 10µg/mL Aprotinin, 5µg/mL leupeptin, 1mM DTT) for 15 minutes to induce cell swelling. Cells were lysed with 50µl of 10% Nonident P-40 and vortexed for precisely 30 seconds. Lysates were microcentrifuged for 30 seconds at 16,000 x g to collect the nuclei. Nuclear pellets were then resuspended in 75µl "Buffer C" (400mM NaCl, 7.5mM $MgCl_2$, 0.2mM EDTA, 0.1mM EGTA, 1mM PMSF, 1mM DTT, 25% glycerol (v/v), 10µg/mL Aprotinin, 5µg/mL leupeptin) by shaking for 15 minutes on ice, and the supernatant collected by centrifugation for 1 minute at 4^{o}C. The supernatant, containing the nuclear extract, was collected and frozen at -80^{o}C.

2.6.14 RCDC Protein Estimation

The protein concentration of all cell extracts was determined using the RCDC Protein Assay Kit (BioRad, USA) according to manufacturer's instructions. Serial dilutions of BSA (2mg/mL stock) were used to create a standard curve.

2.6.15 Protein Detection -Western Immunoblotting

Laemmli SDS-PAGE gels were made according to established protocols [409]. Prior to loading of whole cell lysates, samples were boiled for 5 minutes at 100^{o}C and then centrifuged at maximum speed for 5 minutes at 4^{o}C. The proteins were then loaded on 8-10% SDS PAGE gels and run in SDS running buffer (0.3% (w/v) Tris-HCl, 1.44% (w/v) Glycine, 0.1% (w/v) SDS in water) at 20mA until the bromophenol blue buffer front entered the separating gel, and then at 30mA until the dye front had migrated to the end of the gel. Gel electrophoresis was performed using the BioRad Mini-PROTEAN® III System (BioRad, USA)

Following SDS-PAGE gel electrophoresis, proteins were transferred to a PVDF nitrocellulose membrane (Amersham, UK) using the BioRad Mini Trans-Blot® Electrophoretic Transfer System (BioRad, USA) in SDS-PAGE transfer buffer (0.3% (w/v) Tris-HCl, 1.44% (w/v) Glycine, 15% Methanol (v/v), 0.1% SDS) at 30mA overnight.

Following removal from the transfer apparatus, the nitrocellulose membrane was rinsed briefly in Tris-buffered saline (TBS), and blocked in TBS-Tween 20 (TBS-T, TBS supplemented with 0.05% (v/v) Tween 20) supplemented with 2.5% (w/v) casein blocking reagent (Amersham, UK) and 1% BSA for 8 hours on a rocking platform at RT. The membrane was incubated in the primary antibody (diluted 1:1000 in TBS-T) overnight at 4^{o}C on a rocking platform.

The membrane was rinsed briefly in TBS-T and then washed thoroughly three times for 5 minutes in TBS-T at RT on a platform shaker. The membrane was then probed with a biotinylated secondary antibody (diluted 1:2000 in TBS-T) for 1 hour at RT on a platform shaker. The secondary antibody solution was removed and the membrane washed as described above. The membrane was then probed with an alkaline phosphatase-conjugated streptavidin (diluted 1:2000 in TBS-T) for 1 hour at RT on a platform shaker, and the membrane was washed as described above. Antibody binding was visualised by enhanced chemiluminescence (ECF, Amersham, UK) as per manufacturer's instructions and scanned on a Typhoon 9410 (Amersham, UK) using 488nm excitation.

2.6.15.1 Antibodies Used In This Study

Table 2.5. Antibodies Used For Western Immunoblotting

Primary	**Details**	**Source**	**Cat. No.**
HIF-1α	Purified mouse anti-human HIF-1α	BD Bioscience	610959
HIF-2α	Rabbit polyclonal anti-HIF-2α	Novus Biologicals	NB-100-122
α-tubulin	Rat monoclonal anti-α-tubulin	Abcam	ab6160
Secondary	**Details**	**Source**	**Cat. No.**
Anti-mouse	Goat anti-mouse IgG-biotin	Southern Biotechnologies	1030-08
Anti-rabbit	Biotinylated rabbit IgG	Vector Lab	CA-1000
anti-rat-ALP	Goat anti-rat IgG-alkaline phosphatase	Chemicon	AP136A
Tertiary	**Details**	**Source**	**Cat. No.**
SAV-ALP	Streptavidin-alkaline phosphatase	Amersham	RPN1234

2.6.16 Electrophoretic Mobility Shift Assay (EMSA)

2.6.16.1 Oligonucleotide and 32P-labelled Probe Preparation

The oligonucleotide for "HIF Binding Site 1" of the CXCL12 promoter (5'-GGGACAGGGACGTGTCCCCAGGG-3') was purchased from Geneworks (Australia) and full-length product purified from non-denaturing polyacrylamide gels according to established protocols [410]. Briefly, single-stranded DNA probes were prepared by end-labelling 100ng of oligonucleotide with T4 polynucleotide kinase and [γ-^{32}P] ATP in a 10μl reaction. The reaction was incubated for 1 hour at 37^{o}C, and allowed to cool prior to the annealing of the complementary oligonucleotide (5'-CCCTGGGGACACGTCCCTGTCCC-3') at 95^{o}C for 5 minutes. Formamide load buffer (80% (w/v) deionised formamide, 0.01% (w/v) bromophenol blue, 0.01% (w/v) xylene cyanol, 0.1mM EDTA in 0.5x TBE buffer) was added and full length end-labelled oligonucleotide separated on 10-12% non-denaturing polyacrylamide gel, exposed to X-ray film, the bands excised and oligonucleotide eluted from the gel in 200μl of TE buffer overnight at 4^{o}C.

2.6.16.2 Preparation of cellular extracts

Cell extracts for EMSAs were prepared according to published protocols [298]. Briefly, cells were harvested and centrifuged at 400 x g for 5 minutes. The cell pellet was washed once with PBS and then resuspended in 4 packed cell volumes (200µl) of "Buffer A" (10mM Tris-HCl, pH 7.5, 1.5mM $MgCl_2$, 10mM KCl, 1mM DTT, 0.4mM PMSF, 1mM $NaVO_4$, 1x Protease Inhibitor Cocktail) and incubated on ice for 10 mins. Cell nuclei were liberated by addition of 50µl of 10% NP-40 and vortexed for 30 seconds. Nuclei were pelleted by centrifugation at 10,000 x g for 2 mins at 4°C and then resuspended in 3 packed cell volumes (100µl) of "Buffer C" (0.42M KCl. 20mM Tris-HCl, pH 7.5, 20% v/v glycerol, 1.5mM $MgCl_2$, 1mM DTT, 0.4mM PMSF, 1mM $NaVO_4$, 1x Protease Inhibitor Cocktail). After rotation for 30 mins at 4°C, samples were centrifuged for 30 mins at 15,000 x g at 4°C and supernatant collected. 100µl of "Dialysis buffer" (20mM Tris-HCl, pH 7.8, 100mM KCl, 0.2mM EDTA, 20% glycerol, 1mM DTT, 0.4mM PMSF, 1mM $NaVO_4$, 1x Protease Inhibitor Cocktail) was added to this supernatant, dialysed using Nanosep 10K spin columns (Pall Corporation, USA).

2.6.16.3 EMSA analysis

Binding reactions were performed using 0.25ng of double-stranded ^{32}P-labelled oligonucleotide probes in a 10µl reaction mix containing 10mM Tris-HCl, pH 7.5, 50mM NaCl, 1mM $MgCl_2$, 1mM EDTA, 5mM DTT and 5% glycerol containing 0.25µg poly dIdC and 5µg of nuclear extracts. Reaction mixes were incubated at 4^{o}C for 30 minutes and load buffer added prior to resolution at 4^{o}C on a pre-electrophoresed 4% non-denaturing polyacrylamide gel in 0.5x TBE buffer at 200V. Gels were then dried and visualised by exposure to a Storage Phosphor Screen (GE Healthcare, USA).

2.6.17 Luciferase Reporter Assays

With the exception of these luciferase reporter assays, all transduced cell lines created in this project contained the SFG-$_{NES}$-TGL luciferase vector (Figure 2.4) to facilitate *in vivo* bioluminescence monitoring. However, as the presence of the SFG-$_{NES}$-TGL vector would confound the data from luciferase reporter assays, it was necessary to use cells lines that lacked the SFG-$_{NES}$-TGL construct. The cell lines that were used in these assays were the unmodified parental LP-1 cell line and LP-1 cells containing the pRUF-IRES-GFP-HIF-1α and pRUF-IRES-GFP-HIF-2α over-expression constructs and the relevant pRUF vector control.

Cells were centrifuged at 400 x g for 5 minutes at 4°C and the pellet resuspended to 4.5 x 10^6 cells per 500µl in RPMI medium supplemented with 20% FCS. DNA was added to electroporation cuvettes (5µg of reporter plasmid and 10µg of expression plasmid) then the cells were added and the cell/DNA mix was allowed to sit for 10 minutes prior to electroporation. Electroporation was performed using a Bio-Rad Gene Pulser at 270V and a capacitance of 960µF. Following electroporation, the cells were left to rest for 10 minutes, then 1mL of RPMI medium was added, and the entire contents of the cuvette transferred to a tissue culture flask with 9mL of RPMI-10. The cells were incubated for 24 hours in a humidified environment at 37°C in the presence of 5% CO_2. Transfected cells were then subjected to normoxic or hypoxic culture conditions for 48 hours, and then assayed for luciferase activity. Cells were centrifuged at 400 x g for 5 minutes at 4°C and then washed twice with PBS. The resultant pellet was then resuspended in 200µl of "Lysis Buffer" (100mM potassium phosphate buffer, 2mM DTT, 0.01mM EDTA in Milli-Q water) and freeze-thawed three times using liquid nitrogen and a 37°C water bath. Cellular debris was pelleted by centrifugation for 5 minutes at 16,000 x g and the protein concentration determined using the RCDC reagent (Section 2.6.14).

Using a 96-well black Packard Lite-Plate™, 200µl of "Luciferase Assay Buffer" (100mM potassium phosphate buffer, 2mM DTT, 10mM MgSO4, 320mM Coenzyme A, 500mM ATP in Milli-Q water) was added into the appropriate wells and then 20µg of protein extract added. Immediately prior to analysing the plate in a Packard Topcount Luminometer, 40µl of 1mM D-Luciferin (Roche, USA) was added to each well. Luminescence was measured in counts per second and all values were compared to the empty vector.

2.6.18 Chromatin Immunoprecipitation (ChIP)

ChIP assays were performed using a commercial EZ-Magna ChIP™-G kit (Millipore, USA) according to the manufacturer's instructions. Briefly, 1 x 10^7 LP-1 cells were cultured under normoxic or hypoxic culture conditions for 48 hours. Cells were cross-linked with freshly prepared 1% formaldehyde for 10 min at RT, which was then quenched with 125mM glycine for 5 minutes at RT. Cells were washed three times in ice-cold PBS, lysed sequentially in 500µl "Lysis Buffer" and 500µl "Nuclear Lysis Buffer" containing protease inhibitors, and sonicated for 30 minutes (30s pulses with 30s rest periods) using a BioRuptor™ waterbath sonicator (Diagenode, Belgium) to shear the cross-linked DNA

into ≈200-1000bp fragments. For each immunoprecipitation, 50µl of sheared cross-linked chromatin was diluted to a final volume of 500µl in "Dilution Buffer" containing protease inhibitors and incubated with 20µl magnetic beads and 5µg primary antibody overnight at 4°C on a rotating platform. The primary antibodies used were anti–HIF-2α (NB100-132; Novus Biologicals Inc.), anti–HIF-2α (NB100-122; Novus Biologicals Inc.), anti-HIF-2α (ab199, Abcam), their corresponding isotype-matched negative controls, and anti-RNA polymerase II as a positive control (provided with the kit). The next day, the DNA/protein/antibody complexes were collected using a magnetic particle collector, washed sequentially in "Low Salt Buffer", "High Salt Buffer", "LiCl Buffer" and "TE Buffer" for 5 minutes each with rotation, then eluted with 100µl "Elution Buffer" containing 100ug/mL Proteinase K at 62°C for 2 hours with rotation. Reactions were incubated at 95°C for 10 minutes to reverse the protein/DNA cross-links and free the DNA, and the eluted DNA was separated from the magnetic beads using a magnetic stand. Eluted DNA was purified using spin columns, and subjected to PCR analysis using primers designed to amplify the two HIF binding sites (HBS) on the CXCL12 promoter as detailed in Table 2.6 (see also Appendix 1).

Table 2.6. ChIP Primers Used In This Study

Target	Forward Primer (5'-3')	Reverse Primer (5'-3')
CXCL12 HBS #1[§]	TCTAACGGCCAAAGTGGTTT	GCCACCTCTCTGTGTCCTTC
CXCL12 HBS #2[§]	TCCGTGGGAAGAGTTTTCTG	GGACGGGAGATTCAATGAGA

[§] Sequence from Ceradini *et al*, 2004, Nature Medicine, 10(8): 858-864.

2.7 Retroviral Transfection and Infection Techniques

2.7.1 Cloning and Expression Vectors

(a) pRUF-IRES-GFP (Figure 2.2) – a 5950 base pair MMLV-based retroviral vector was a kind gift from Mr Paul Moretti (Hanson Institute, South Australia). This vector was used to create the HIF-1α, HIF-2α and CXCL12 over-expressing cell lines.

(i) pRUF-IRES-GFP-HIF-1α - The HIF-1α coding region (a kind gift from Associate Professor Dan Peet, University of Adelaide) was excised from pBLUESCRIPT-HIF-1α using *Sma*I and *Hpa*I enzymatic digestion, blunt-

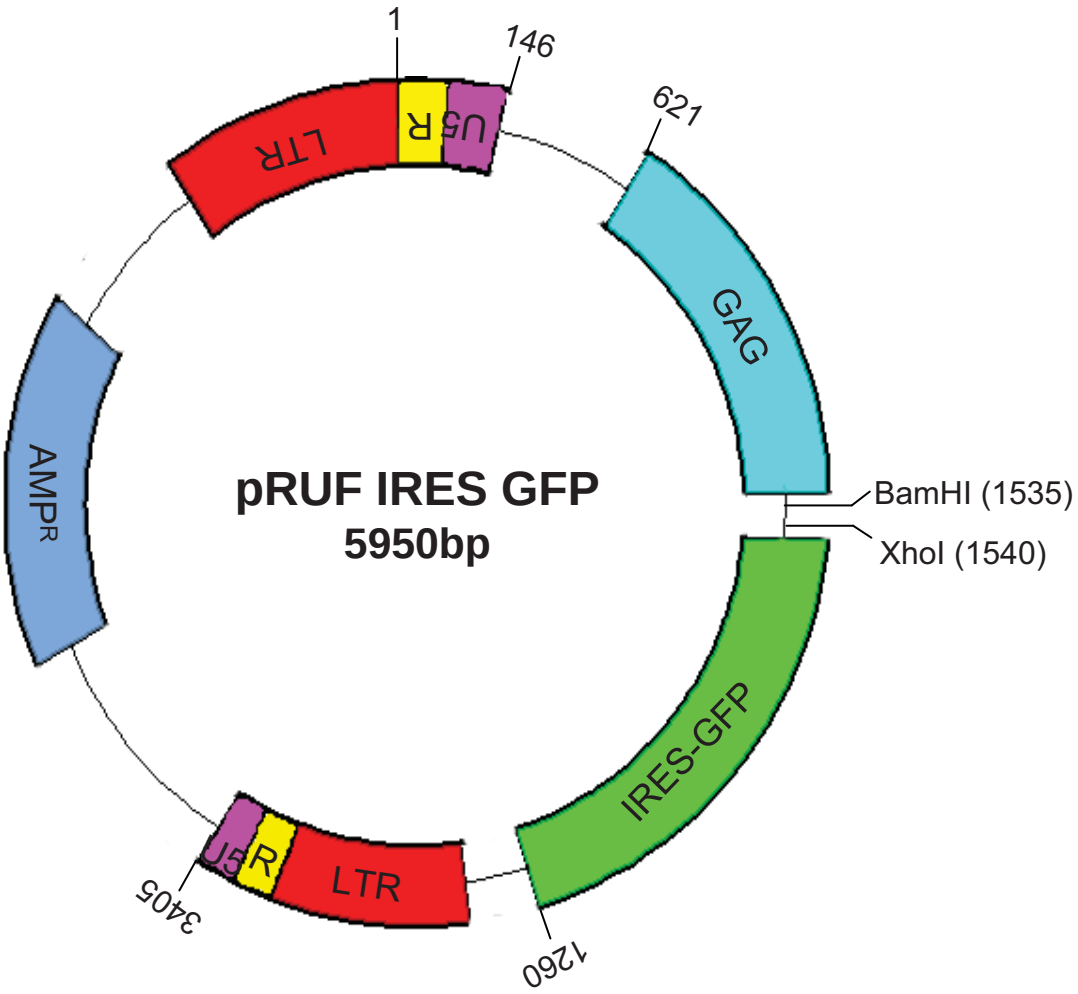

Figure 2.2. The pRUF-IRES-GFP Mammalian Expression Vector. This 5950bp retroviral vector was used to create the HIF-1α-, HIF-2α- and CXCL12- over-expressing cell lines.

ended using Klenow fragment and ligated into the pRUF-IRES-GFP vector, which had been digested with *Bam*HI.

(ii) pRUF-IRES-GFP-HIF-2α - The HIF-2α coding region (a kind gift from Associate Professor Dan Peet, University of Adelaide) was excised from pefbos-HIF-2α using *Bam*HI enzymatic digestion, blunt-ended using Klenow fragment and ligated into the pRUF-IRES-GFP vector which had been digested with *Bam*HI.

(iii) pRUF-IRES-GFP-CXCL12 – The CXCL12 coding region was excised from pLNCX2-CXCL12 using *Xho*I and *Sal*I enzymatic digestion and ligated into the pRUF-IRES-GFP vector, which had been digested with *Xho*I.

(b) pFIV-H1-cop-GFP (Figure 2.3) – a 6339 base pair lentiviral vector which was purchased from System Biosciences (Cat. No. #SI111A-1, USA). This vector was used to create all of the HIF-1α, HIF-2α and CXCL12 RNAi cell lines (Section 2.7.2.1 and Section 2.7.2.2 below).

(c) SFG-$_{NES}$-TGL (Figure 2.4) – an approximately 10,000 base pair vector which was a kind gift from Dr Vladimir Ponomarev [411] (Department of Radiology, Memorial Sloan Kettering Cancer Centre, New York, USA). This vector was co-transfected into all stably infected cell lines to facilitate *in vivo* bioluminescence monitoring.

(d) pGL3 basic (Figure 2.5) – a 4818 base pair vector which was purchased from Promega (Cat. No. #E1751, USA). This vector was transiently transfected into cells for luciferase reporter assays.

(i) pGL3b-CXCL12 – The proximal CXCL12 promoter was PCR amplified from genomic LP-1 DNA using primers containing enzymatic restriction sites for *Hind*III and *Xho*I (see below, restriction sites underlined. See also Appendix 1). This resultant DNA was purified with the AquaPure Genomic DNA Isolation kit (BioRad, USA). The CXCL12 promoter region was excised from this purified DNA using *Hind*III and *Xho*I enzymatic digestion and ligated into the pGL3b vector, which had also been digested with *Hind*III and *Xho*I.

5’-GCGCTCGAGCCATCTAACGGCCAAAGTGG-3’ (*Xho*I)

5’-GCGAAGCTTGGCTGACGGAGAGTGAAAGTG-3’ (*Hind*III)

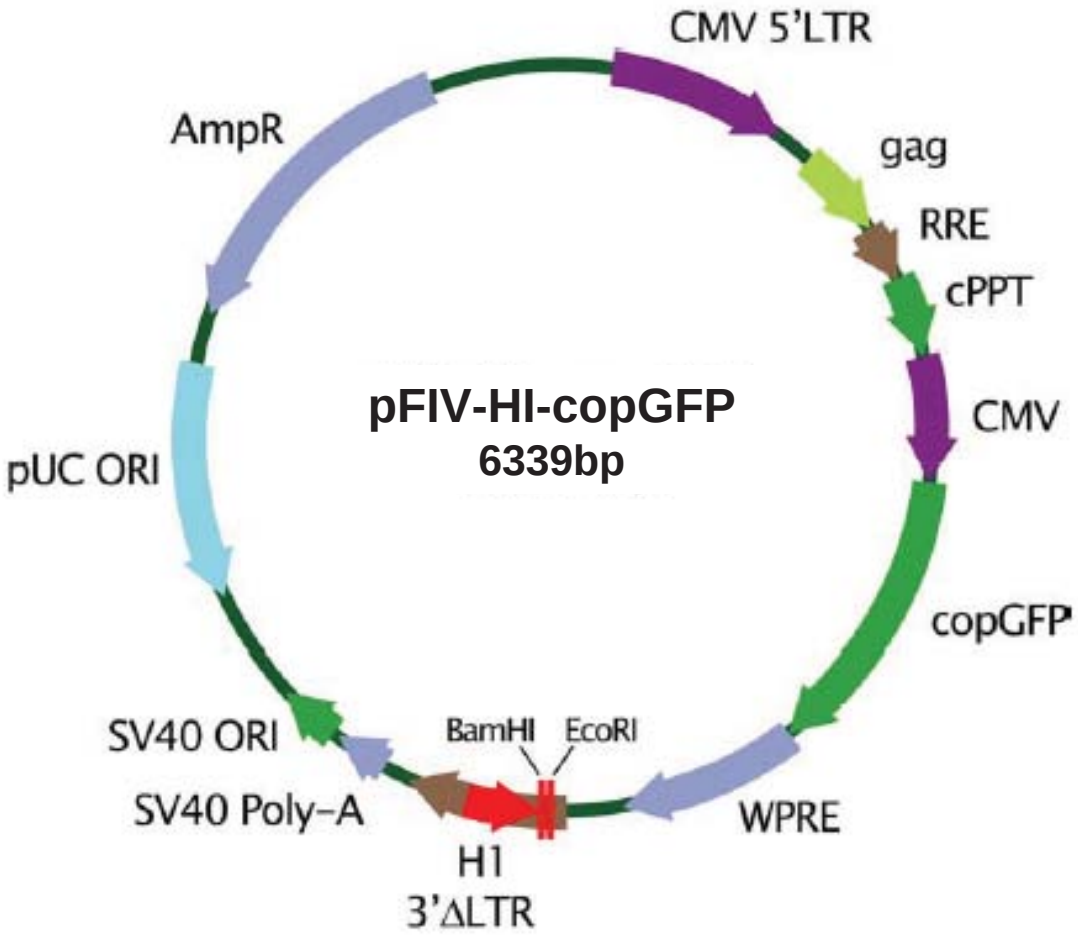

Figure 2.3. The pFIV-H1-copGFP Mammalian Expression Vector. This 6339bp lentiviral vector was used to create the HIF-1α-, HIF-2α- and CXCL12- knockdown cell lines.

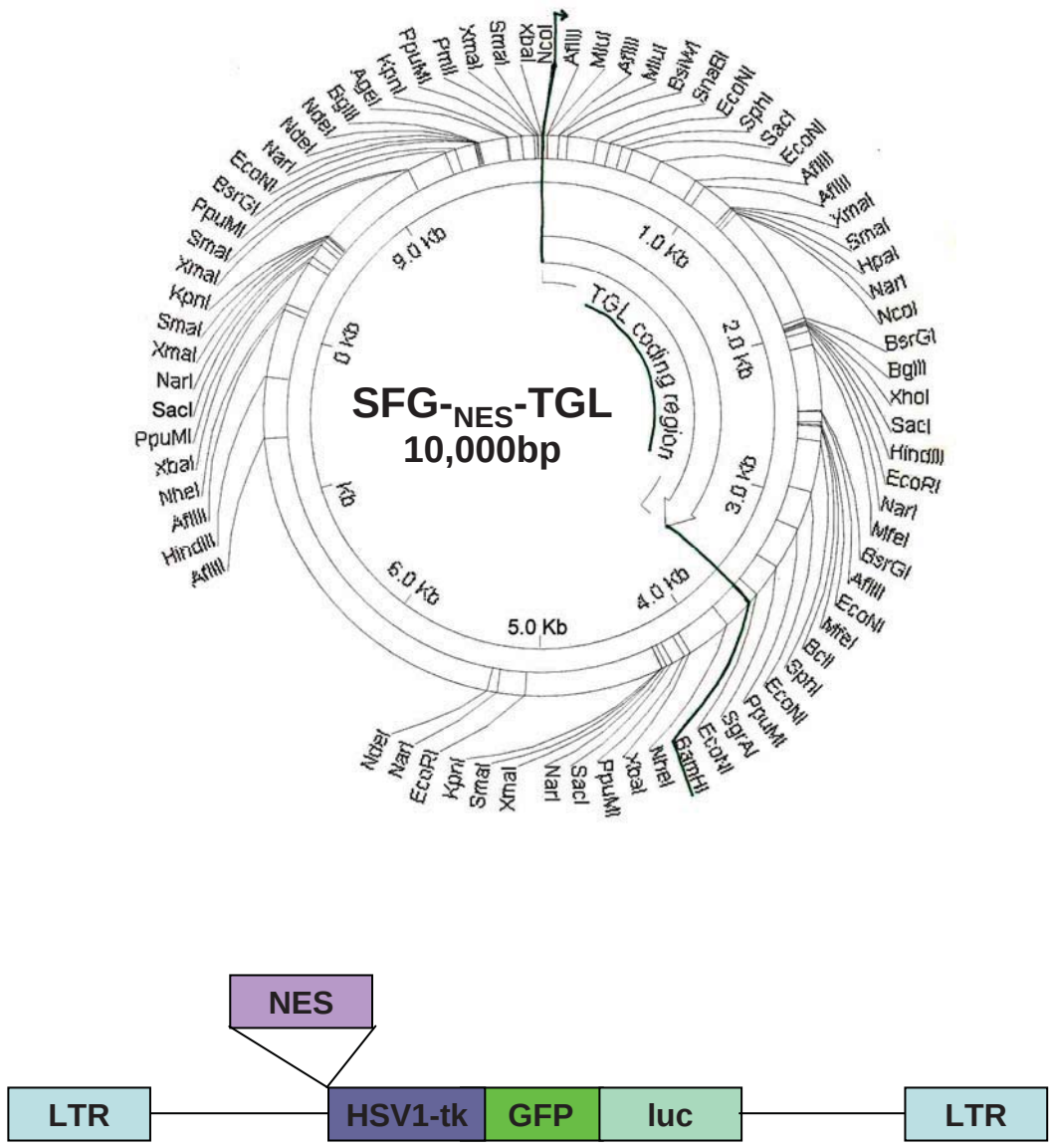

Figure 2.4. The SFG-$_{NES}$-TGL Mammalian Expression Vector. This 10,000bp vector was co-transfected into all stably-transduced cell lines to facilitate *in vivo* bioluminescence monitoring.

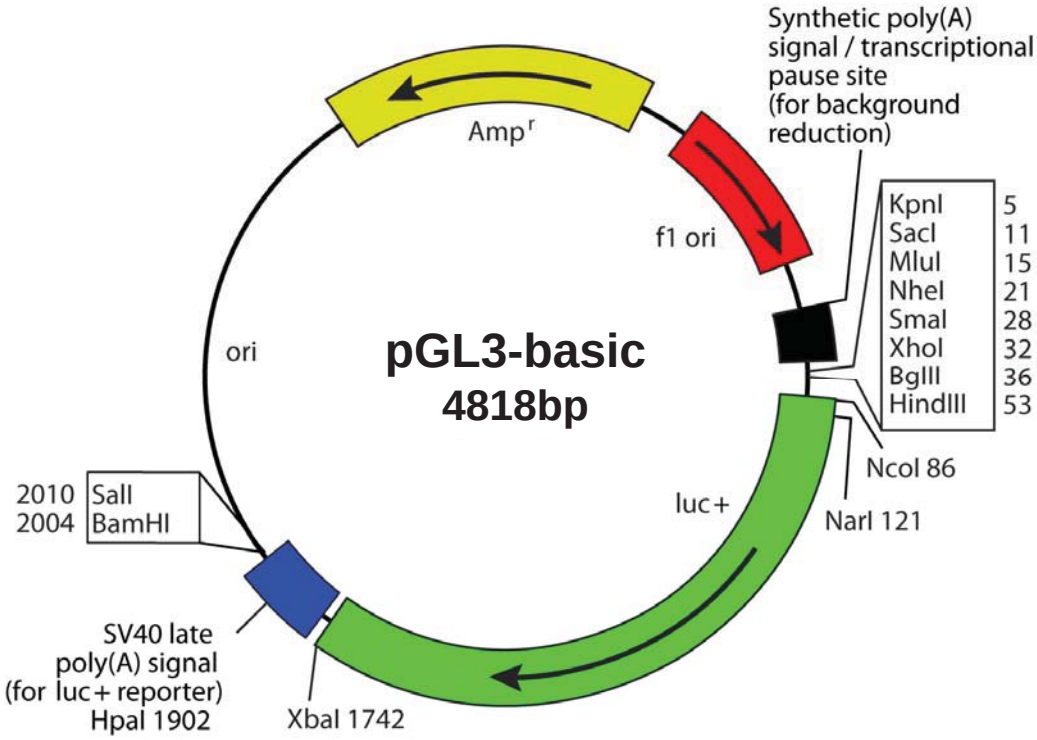

Figure 2.5. The pGL3-basic Mammalian Expression Vector. This 4818bp vector was transiently transfected into cells for luciferase reporter assays.

2.7.2 Synthetic RNAi Knockdown Oligonucleotides for Retroviral Packaging

2.7.2.1 HIF-1α and HIF-2α RNAi

The oligonucleotides for the HIF RNAi constructs were designed to conform to the structure presented in Figure 2.6 below.

Figure 2.6. Structure of the RNAi Constructs

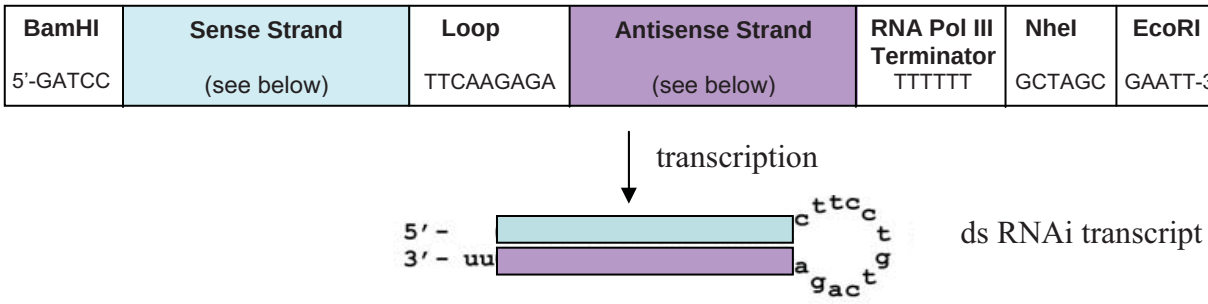

The 'Sense Strand' and 'Antisense Strand' sequences (highlighted in blue and purple in the above diagram) are detailed in Table 2.7.

Table 2.7. HIF RNAi Oligonucleotides Used in This Study

Target	'Sense Strand' Sequence (5'-3')	'Antisense Strand' Sequence (5'-3')
HIF-1α #1[§]	CCATGAGGAAATGAGAGAAATGCTT	AAGCATTTCTCTCATTTCCTCATGG
HIF-1α #2[♣]	AACTAACTGGACACAGTGTGT	ACACACTGTGTCCAGTTAGTT
HIF-1α scrambled[§]	CCAAGGAGTAAGAGATAAAGGTC	GACCTTTATCTCTTACTCCTTGG
HIF-2α #1[‡]	GACAAGGTCTGCAAAGGGTT	AACCCTTTGCAGACCTTGTC
HIF-2α #2[‡]	GGGGGCTGTGTCTGAGAAGAGT	ACTCTTCTCAGACACAGCCCCC

[§] Sequence from Solban *et al*, 2006, Cancer Research, 66(11): 5633-5640.
[♣] Sequence from Marxsen *et al*, 2004, The Biochemical Journal, 381(3): 761-767.
[‡] Sequence from Zimmer *et al*, 2004, Molecular Cancer Research, 2(2): 89-95.

2.7.2.2 CXCL12 RNAi

The CXCL12 RNAi construct was designed with the following structure and transcribed into the same hairpin loop conformation as the HIF RNAi constructs (depicted in Figure 2.6) except with a different loop sequence.

BamHI	Sense Strand	Loop	Antisense Strand	RNA Pol III Terminator	EcoRI
5'-GATCC	(see below)	CTTCCTGTCA	(see below)	TTTTT	GAATT-3'

The 'Sense Strand' and 'Antisense Strand' sequences (highlighted in pink and yellow in the above diagram) are detailed in Table 2.8, and were designed for us by SBI.

Table 2.8. CXCL12 RNAi Oligonucleotide Used in This Study

Target	'Sense Strand' Sequence (5'-3')	'Antisense Strand' Sequence (5'-3')
CXCL12 #2	GCCAGTTGGATGGGAATTTGAGTGTT	GAAGCACTCAAATTCTCATCCAGCTGG

2.7.3 Transfection of HEK-293T Packaging Cell Line with GFP-Encoding Plasmids

Twenty four hours prior to transfection, 6cm tissue culture dishes were seeded with 1 x 10^6 HEK-293T cells in a volume of 3mL of DMEM-10 (equating to approximately 50-60% confluency on the day of transfection) and incubated in a humidified environment at 37^{o}C in the presence of 5% CO_2. At the time of transfection, the media was removed from the dishes and replaced with 2mL of DMEM-10. The following two mixtures were prepared for each 6cm tissue culture dish – Mix 1: 5μg retroviral GFP plasmid DNA, 4μg pGP plasmid (encoding GAG and Pol), and 4μg pVSVG plasmid (encoding viral envelope protein) in 500μl serum-free DMEM; Mix 2: 20μl Lipofectamine 2000 (Invitrogen, USA) added drop-wise to 500μl serum-free DMEM. Mix 2 was incubated at RT for 5 minutes, then added drop-wise to Mix 1. This DNA/Lipfectamine mixture was incubated for a further 20 minutes at RT, at which point it was added drop-wise to the HEK-293T cells. The cells were incubated in a humidified environment at 37^{o}C in the presence of 5% CO_2 for 48 hours, and the efficiency of the transfection was assessed under a UV microscope (Olympus, Japan).

2.7.4 Viral Infection of Cells

At 48 hours post-transfection, the supernatant from the HEK-392T cells (containing viral particles) was filtered through a 0.45μm low protein binding syringe filter (Nalgene, USA) to remove any cellular debris, diluted 1:1 with fresh media (in which the cells to be infected are grown) and 4μg/mL polybrene (Sigma, USA) was added immediately prior to its addition to the cells. The cells (non-adherent) to be infected were plated at 2 x 10^5 cells/mL. Forty eight hours after viral infection, the viral supernatant was removed, and the cells were cultured in their normal growth medium. GFP expression was assessed using a UV microscope (Olympus, Japan). The infected cells were then sorted for GFP expression

using a Coulter EPICS ALTRA flow cytometer (Beckman Coulter, USA), with the top 30% of GFP positive cells selected for the generation of transduced cell lines.

2.7.5 Creation of Clonal Populations of Virally Infected Cells

To generate satisfactory levels of HIF-1α, HIF-2α and CXCL12 knockdown in stably-infected cells, it was necessary to create clonal cell lines. The previously-sorted cells were re-sorted using a Coulter EPICS ALTRA flow cytometer (Beckman Coulter, USA), and single cells deposited into a 96-well plate from the top 10% of GFP expressing cells. These single-cells were cultured until they had expanded enough to assess the level of knockdown by real-time PCR and western immunoblot analyses.

2.8 Statistical Analysis

Data points are reported as the mean ± standard error of the mean (SEM). Analysis of the variance to determine significant differences between treatments was performed using a one-way ANOVA with Dunnett's post-hoc test, or Pearson Product Moment test on the SigmaStat® 3.0 software package (Systat, USA). Statistical significance was determined for a two-tailed test and H_o (null hypothesis, $\mu = \mu_o$) was rejected at significance $p \leq 0.05$. Each experiment was repeated at least three times for these analyses.